AUSTRALIAN TRANSPORT SAFETY BUREAU

DOCUMENT RETRIEVAL INFORMATION

Title and Subtitle

Development of an Anti-Whiplash Seat

Authors

Michael Yuen, Mr.

Lynne E. Bilston, Dr.

Performing Organisation

The Prince of Wales Medical Research Institute
Barker St. Randwick NSW 2031 Australia

Sponsored by / Available from

Australian Transport Safety Bureau
GPO Box 967
CANBERRA ACT 2608

Project Officer: John Collis

Abstract

This project involved the development of an anti-whiplash car seat for rear impact collisions. Concept seat models were created in MADYMO and rear impact simulations with a seated THOR dummy were conducted. The process involved modifying seat geometry to determine the optimal seatback and head restraint configuration. The intention was to minimise head, neck and T1 accelerations, angles and NIC values. The final design includes a new seatback design that keeps the upper seatback within close proximity to the upper torso.

The concept seat was constructed by modifying the seatback and head restraint of an existing production seat. The design can be configured as a concept seat and a standard seat both with and without an active head restraint. Rear impact sled tests with a THOR and a BioRID dummy were conducted to compare the performance of both the concept seat and the standard seat.

Analysis included comparison of head and T1 peak accelerations, angles and NIC values. The results for the concept seat show a significant improvement over the standard seat. The implementation of an active head restraint further reduces the injury potential. This project showed that injury potential can be reduced significantly with the implementation of an occupant conforming seatback and active head restraint.

Keywords

Whiplash injury; Rear Impact; Seat Design; Injury prevention

ACKNOWLEDGMENTS

The authors wish to thank the Australian Transport Safety Bureau for funding this project. In addition, thanks to the Department of Transport and Regional Services for the loan of their THOR dummy, the RTA CRASHLAB for technical advice and the loan of Hybrid III arms, Subaru Australia for the supply of seats, the Prince of Wales Medical Research Institute workshop and the Ian Potter foundation for funding equipment.

TABLE OF CONTENTS

EXECUTIVE SUMMARY

This project involved the development of an anti-whiplash car seat for rear impact collisions. The extent of whiplash related injuries can be reduced by controlling the occupant motion with the seatback and head restraint. Current production seats attempt to optimise the seat configuration but are usually only suitable for an upright seating position. When the seatback becomes more reclined through manual adjustment by the occupant or through torso loading during a rear impact, the distance between the head restraint and the head increases. This increase in distance increases the amount of differential motion between the head, neck and torso.

Concept seat models were created in MADYMO and rear impact simulations with a seated THOR dummy were conducted. The process involved modifying seat geometry to determine the optimal seatback and head restraint configuration. The intention was to minimise head, neck and T1 accelerations, angles and NIC values. The final design includes a new seatback design that keeps the upper seatback within close proximity to the upper torso.

The concept seat was constructed by modifying the seatback and head restraint of an existing production seat. The design can be configured as a concept seat and a standard seat both with and without an active head restraint. Sled testing of the concept seat against the standard seat was conducted with both a THOR and a BioRID dummy. The THOR dummy was used throughout the design phase of the project while the BioRID dummy, a rear impact specific dummy, was used for final validation of the concept seat design.

Analysis included comparison of head and T1 peak accelerations, angles and NIC values. The results for the concept seat show a significant improvement over the standard seat for all parameters. The implementation of an active head restraint further reduces the injury potential. With both the new seatback and active head restraint in use a NIC value of $12.2m^2/s^2$ was recorded for a 15 degree seatback angle. For a 25 degree seatback angle the NIC value was $11.6m^2/s^2$. The NIC value for the standard seat with a fixed head restraint was $28.9m^2/s^2$ for the 15 degree case and $31.8m^2/s^2$ for the 25 degree case. It should be noted that the current threshold value is $15m^2/s^2$. No injury is likely to occur if the NIC value can be maintained below this threshold. While the NIC for the standard seat exceeds the threshold by as much as $16.8m^2/s^2$, the NIC for the concept seat with active head restraint remains below the threshold.

Sled tests with a BioRID dummy revealed that the NIC value for a 15 degree standard seat with a fixed head restraint could be reduced by 6.9% when an active head restraint was implemented. The new seatback design with a fixed head restraint reduces the NIC value by 44.6%. Similarly for the 25 degree standard seat with a fixed head restraint where the use of an active head restraint reduces the NIC value by 18.24% while the new seatback design reduces the NIC value by 51.9%. When the active head restraint is used with the new seatback design the NIC values are reduced by 57.8% for the 15 degree seatback angle and 63.5% for the 25 degree seatback angle. These results clearly show the whiplash reduction potential of the new seatback design is more significant than that of the active head restraint alone.

The completion of this project has shown that the whiplash injury potential during rear impact can be significantly reduced with the implementation of an occupant conforming seatback that maintains an optimal position for any seatback angle. This result was enhanced by the addition of an active head restraint.

CHAPTER 1 - BACKGROUND AND PROJECT SCOPE

1.1 BACKGROUND

1.1.1 Whiplash Associated Disorders

Whiplash associated disorders are not considered life threatening, however they are associated with long-term consequences that cause human suffering and cost to society (Jakobsson et al. 2002). Hypotheses for whiplash related neck injury mechanisms include the spinal fluid pressure theory (Aldman 1986) and the facet joint damage theory (Bogduk et al. 1988). While the actual cause of whiplash injury is uncertain, researchers agree that the injury is likely to occur during the initial phase of extension as opposed to the rebound phase. Head and neck motion during extension in a rear impact can be categorised into four main phases: initial position, s-shape, extension and hyper-extension (See Figure 1.1). During a rear impact the torso is accelerated forward by the seat back while the head lags behind due to inertia. The head begins to translate with the lower neck in extension and the upper neck in flexion. This phase is commonly described as the s-shape. Once the translation is complete, the head begins to rotate back in extension. The head will continue to rotate and reach a hyper-extension phase if no head restraint contact occurs.

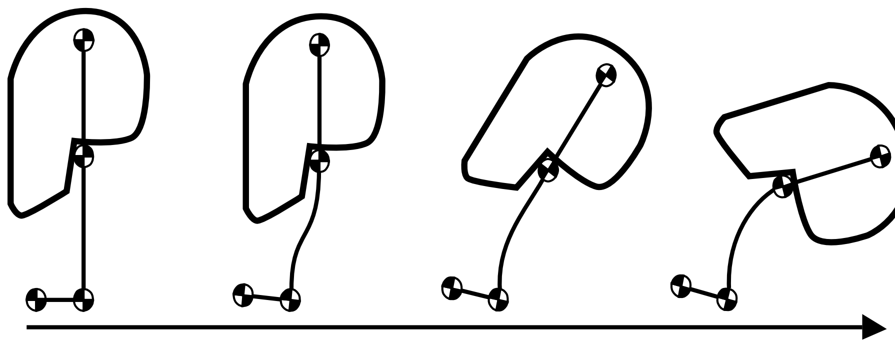

Figure 1.1: Phases of head and neck motion during extension (Figure adapted from Bostrom et al. (1998)). Phase 1 is the pre-impact initial position. Phase 2 is the s-shape phase where the head translates with the lower neck in extension and the upper neck is flexion. Phase 3 is the extension phase where the upper neck has changed from flexion to extension. Phase 4 is the hyper-extension phase that results if no head restraint contact is made.

1.1.2 Crash Test Dummies and Sleds

Rear impact work is generally conducted on crash sleds at low speeds with crash test dummies to simulate a rear impact collision. The most commonly used dummy is the Hybrid III 50th percentile male (Philippens et al. 2002). This dummy was developed for high-speed frontal impacts but has been used in some low-speed rear impact work. Studies have revealed that the Hybrid III dummy shows a poor biofidelic response when compared to human volunteer data (Davidsson et al. 1999). Rear impact work in Australia is currently limited to the use of Hybrid III dummies, due to the lack of availability of specialist rear impact dummies, due to the lack of availability of specialist rear impact dummies.

The THOR dummy was developed by GESAC for the National Highway Traffic Safety Administration (Rangarajan et al. 1998). The initial design was for an advanced frontal crash test dummy with some omni-directional attributes; however research has been conducted predominantly in high-speed frontal impacts.

The BioRID dummy has been designed specifically for rear impact and has a fully articulated lumbar, thoracic and cervical spine (Philippens et al. 2002). Extensive work has been conducted to improve and validate the BioRID design including comparison testing with human volunteers and a Hybrid III dummy (Davidsson et al. 1999). This dummy is not currently available in Australia.

The Neck Injury Criterion (NIC) (Bostrom et al. 1996) was proposed and based on the spinal canal pressure theory (Aldman 1986) of whiplash. Svensson et al. (1993) conducted pig testing while Eichberger et al. (1998) conducted volunteer and cadaver testing. The NIC was derived from the Navier–Stokes equation, which was applied to a porcine spinal canal. The equation looks at the relative motion between the base of the head and the first thoracic vertebra (T1). The criterion only evaluates the extension phase of rear impact (See Figure 1.1) and the injury threshold is $15m^2/s^2$.

$$NIC(t) = a_{rel}(t) \cdot 0.2 + (v_{rel}(t))^2 \tag{1}$$

where:

$$a_{rel}(t) = a_x^{T1}(t) - a_x^{Head}(t) \tag{2}$$

$$v_{rel}(t) = \int a_{rel}(t)dt \tag{3}$$

$a_x^{T1}(t) =$ The acceleration-time curve measured at the location of the first thoracic vertebra

$a_x^{Head} =$ The acceleration – time curve measured at the location of the head centre of gravity

$0.2 =$ This represents a section of porcine neck in metres

$NIC_{max} =$ The peak value of NIC(t) during the first 150ms of an experiment or prior to the rebound phase

In an attempt to harmonise rear impact sled testing, a test procedure for rear impact sled testing has been proposed by ETH, GDV and Autoliv (Muser et al. 2001). The report outlines suggested test procedures and corridors for two sled pulses. The first pulse (See Figure 1.2) is typical of a rear impact collision where injury is likely to occur. The second pulse (See Figure 1.2) is typical of a rear impact collision where injury is unlikely to occur.

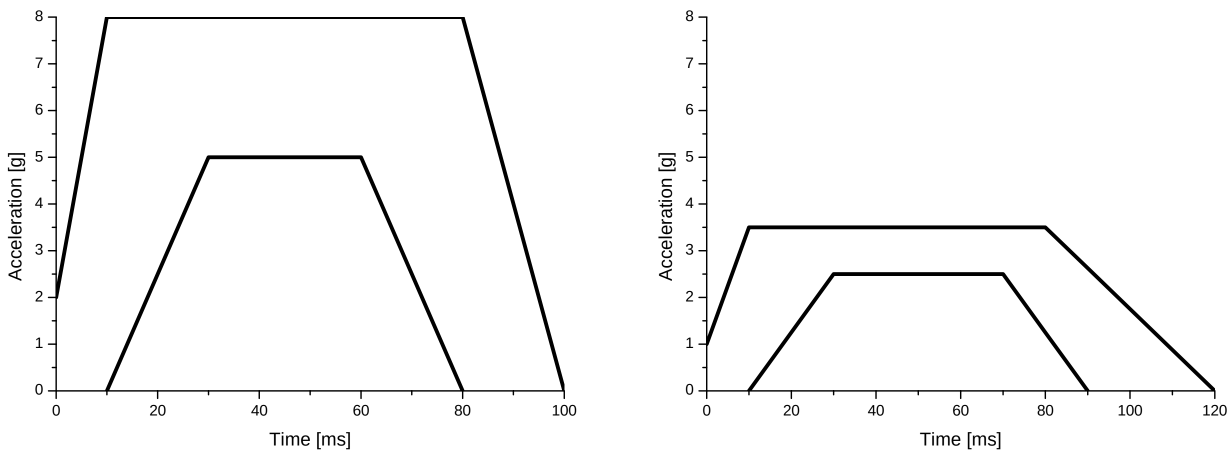

Figure 1.2: Acceleration versus time corridors proposed by Muser et al. (2001).

1.1.3 Anti-Whiplash Seats

Currently, there are two whiplash injury reducing mechanisms available in production car seats. The self-aligning head restraint (SAHR) (See Figure 1.3) was developed by Saab. The design incorporates a gap reducing active head restraint into an otherwise standard production seat. During a rear impact, the torso loads a plate that is located in the upper seat back. The plate is connected to the head restraint through a series of levers. The rearward translation of this plate positions the head restraint further forward and upward with respect to initial position. Subaru have also introduced a seat based on a similar principle.

The Volvo 'WHIPS' seat (See Figure 1.4) was developed in conjunction with Autoliv. The seat was designed to absorb an occupant's kinetic energy during impact. This is opposed to more traditional seat designs where the seatback tends to deflect elastically and then rebound the occupant during impact. A shear pin and lever mechanism is located between the seat back and cushion at the recliner joint. During a rear impact of significant severity, the shear pins fails and allows the seat back to translate towards the rear.

Both the SAHR and WHIPS design are most effective with the seatback set to an upright position. A more reclined seatback angle causes the initial position of the head restraint to move further away and therefore increases the backset. As the seat back angle increases, the rearward torso translation required to activate the head restraint turns into torso ramping up the seatback. On both designs, the front of the head restraint protrudes forward relative to the front of the seatback. While this design minimizes differential motion between the head and torso, there is concern that the head restraint will interfere with the occupants' upper torso and shoulders when torso ramping occurs. Another limitation of the WHIPS design is that the seat must be reset after an impact and new pins must be installed. Furthermore, the seat does not include an active head restraint to help reduce backset during an impact.

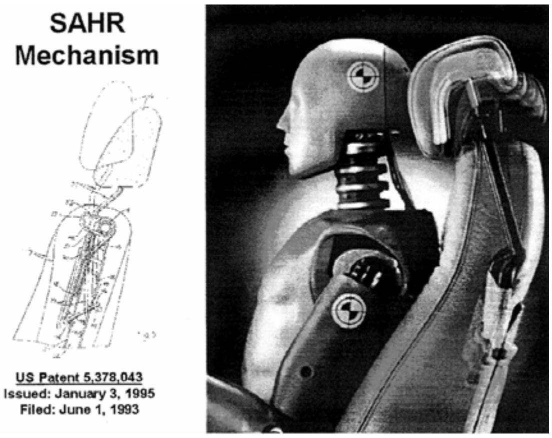

Figure 1.3: Saab seat featuring the Self Aligning Head Restraint mechanism. (From Viano (2001)).

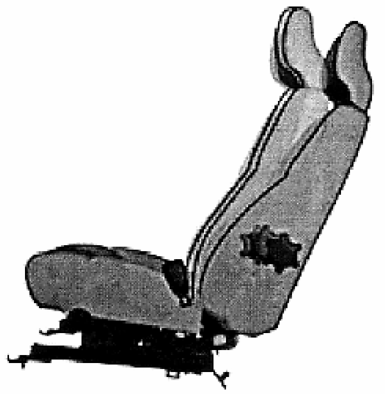

Figure 1.4: Volvo WHIPS seat. Phase 1 involves a rearward translation and phase 2 is a backward tilting motion. (From Jakobsson et al (1998)).

1.2 AIMS

The aim of this project was to develop a whiplash reducing concept seat. The intention was to develop a mechanism that could be incorporated into current production seat designs. The mechanism should maintain a good relationship between the occupant, seatback and head restraint prior to, and during, a rear impact collision and also allow for this to be maintained over a range of seat back angles.

1.3 DESIGN SPECIFICATIONS

Several key factors were considered during the concept seat design:

- The concept seat design should effectively minimise differential motion between the head and neck during a rear impact collision.
- Contact between the occupant and seat should occur earlier to uniformly cushion both the torso and head.
- The design should reduce the injury potential of an occupant regardless of the seat back angle prior to and during a rear impact collision.
- The design should be compatible with production seat dimensions. No protruding components that would increase injury potential to occupants.

- The device should be able to return to pre-impact state after a collision. Mechanical linkages should be used instead of electronic or pyrotechnic devices if possible.
- The device should be practical, economical and manufacturable.
- The device should not induce injury.
- An additional idea was to determine whether it would be advantageous to implement an active type head restraint into the design.

CHAPTER 2 - CONCEPT DESIGNS

2.1 PRELIMINARY WORK

The final concept seat design was influenced by the results of an earlier study that involved rear impact sled tests with a THOR dummy in a rigid seat (Yuen et al. 2003). These tests were conducted to validate a MADYMO alpha THOR model in rear impact. Sled tests with several standard and anti-whiplash production seats were also conducted at this time.

High speed video analysis showed that the distance between the rear of the dummy head and the head restraint, also referred to as the backset, had a major influence on head and neck kinematics as well as the peak accelerations recorded at first thoracic vertebra (T1) and the head centre of gravity. The video analysis also revealed that the torso loads the seatback and causes it to rotate rearwards. Due to the fixed angle relationship between the seatback and head restraint this rearward rotation moves the head restraint further away from the head (See Figure 2.1).

It was also found that production seats that did incorporate some type of active head restraint were only useful at more vertical seat back angles between 10-15 degrees from vertical. As angles approached 25 degrees the active head restraint become less useful. The increased angle is achieved either through initial adjustment by the occupant or by the aforementioned seat back loading via the torso.

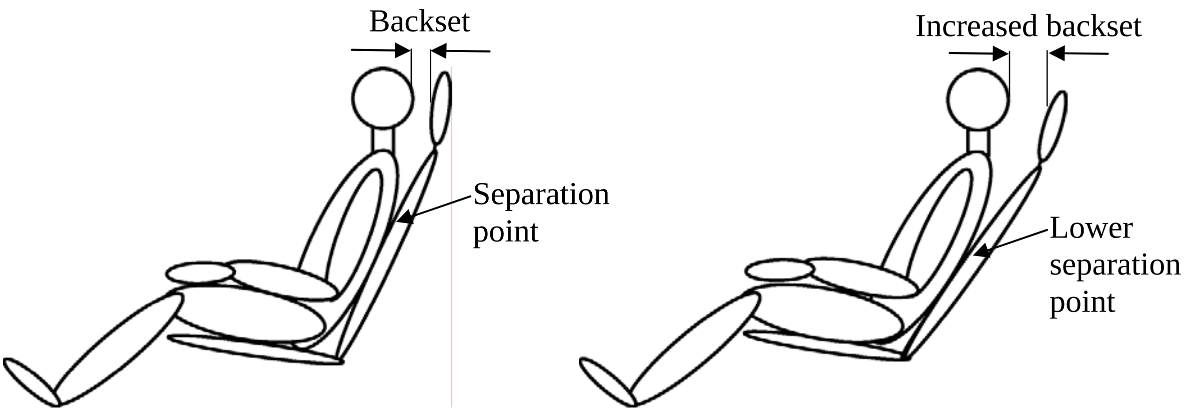

Figure 2.1 – Typical standard production seat schematic. Upright seatback angle on the left and more reclined angle on the right. Most seat designs have been optimised for the upright angle. Note how the fixed angle relationship between seatback and head restraint increases the backset as the seatback angle increases. Also notice the lower separation point on between the torso and seatback for the more reclined seatback angle.

2.2 CONCEPT DESIGN

The initial concept was to develop a backset reducing active head restraint. For vehicle occupants it was observed that as the initial seatback angle increases, the separation point between the upper torso and seat back becomes lower. This is due to the occupant maintaining an upright head and torso posture.

The idea was to develop a seat that conforms to the occupant prior to and during a rear impact at any seatback angle. Initial MADYMO model simulations showed that a modified head restraint would optimise its position relative to the occupants head. The concept seat model showed improved performance over a standard seat model. The results were directly due to the backseat being minimised.

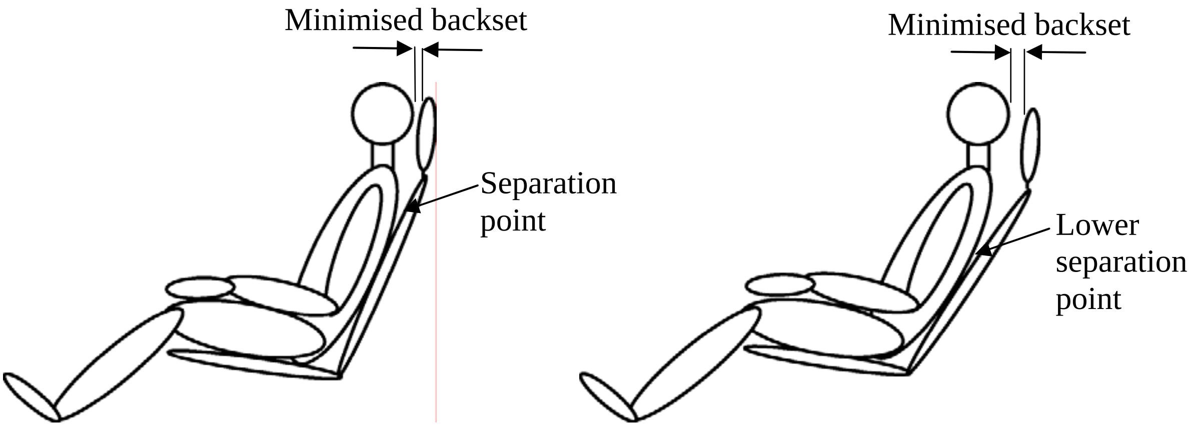

Figure 2.2: Initial concept seat schematic. Upright seatback angle on the left and more reclined angle on the right. This seat design attempts to minimise backset for all seatback angles.

This conforming seatback concept was carried through to the final concept design (See Figure 2.3). Refinements to the design minimised the backset and also the torso to seatback gap. The concept seatback attempts to mimic the curvature of the spine and maintains close proximity to the thoracic spine. The head restraint is also positioned so that height and backset are optimal. Any initial seat back angle will result in a properly adjusted seat configuration. The result is a seat that conforms to the occupant in all seating positions.

The initial idea was to develop some type of active head restraint to minimise backset. Through the preliminary study (See Section 2.1) it was concluded that a typical active head restraint (See Section 1.1.3) would only be useful with an upright seatback angle. Since occupants adjust the seatback to a range of angles and the fact that torso loading during rear impact causes the seatback to rotate, it was concluded that a seat system should be devised to maintain an optimised seatback and head restraint position through a range of seatback angles.

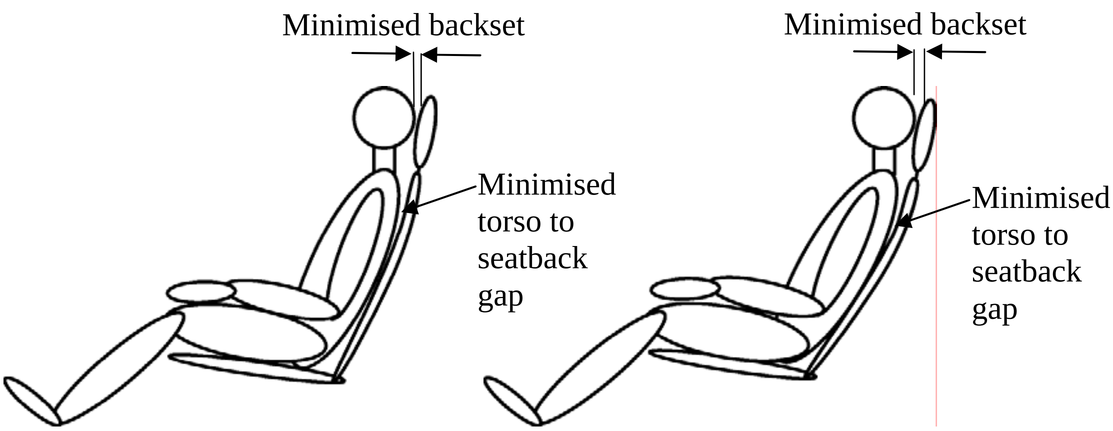

Figure 2.3: Final concept seat schematic. Upright seatback angle on the left and more reclined angle on the right. This seat design attempts to minimise backset for all seatback angles. This seatback design conforms to the natural curvature of the occupant's spine.

CHAPTER 3 - COMPUTATIONAL MODELLING OF SEAT CONCEPT DESIGNS

3.1 RIGID BODY DYNAMIC MODELLING

Rigid body dynamic modelling is used extensively in research and development of new vehicles as well as the analysis of current vehicles in an effort to study and increase safety.

Rigid body modelling involves the creation of tree structures comprised of individual rigid bodies that are connected by kinematic joints. The result is a multibody system that can represent objects such as crash test dummies, car seats and vehicle interiors.

The rigid bodies are defined by attributes such as dimension, mass, inertial properties and joint type. The geometric location of these attributes can also be specified. Joint stiffness, damping and friction can also be specified.

Ellipsoids can be attached to each rigid body to represent the space occupied by each body. Force penetration attributes can be assigned to each ellipsoid to represent contact between various bodies.

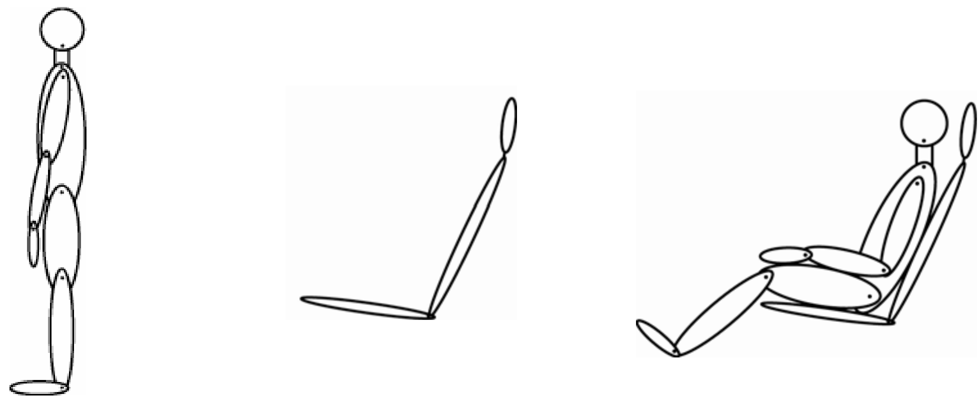

dummy **seat** **seated dummy**

Figure 3.1 – Examples of rigid body models.

Finite element models allow for more detailed and complex models; however the construction of these detailed models is time consuming. Detailed validation is also required. Making changes to these models is also difficult. Furthermore, the time required to solve these models can be large.

In comparison, rigid body modelling packages generally ship with libraries of validated dummies that can be incorporated into a new model. The versatility of the software allows for modifications to be made efficiently. The modified model can then be solved in a matter of minutes. The minimal computation time makes rigid body modelling ideal for research and development work where constant modifications are being made to the multibody systems. For these reasons, multibody dynamic modelling was used as a design tool.

3.2 MADYMO

A multibody dynamics software package called MADYMO was used to develop rigid body concept seat models and simulate rear impact collisions. MADYMO is the most widely used software for crash simulation and includes a library of validated dummies. These dummies can then be inserted into user generated models of the vehicle environment.

A MADYMO model is created in an input data file. The input file structure uses specific keywords that MADYMO recognises during a simulation. The multibody algorithm in MADYMO yields the second time derivatives of the degrees of freedom in explicit form.

A range of output files can be specified such as linear accelerations and relative displacements. This output data can then be converted and analysed with purpose written codes in software such as MATLAB. A kinematics file is also generated and this can be opened with a viewer to inspect simulations graphically.

3.3 MODEL DEVELOPMENT

The first model was a standard production seat with a rigidly attached head restraint (See Figure 3.3). Geometrical and mechanical properties were based on production seat attributes. The seat model featured a tubular steel perimeter frame with ellipsoids attached to the frame to simulate upholstery and allow contact interaction with the dummy. The model was then validated against sled test data. This model was used to study the relationship between the seat back, head restraint and occupant.

Simulations were repeated with a range of seatback angles from 0 to 45 degrees from vertical. This was done to evaluate how different angles would affect head and neck kinematics. The dummy was positioned with an upright torso and a head angle of 0 degrees. With an upright initial seatback angle the backset was 70mm while the torso to seatback distance was 25mm. During impact, the upper torso would contact the seatback before the head would contact the head restraint. The torso loading caused the seatback to rotate rearward and consequently moves the head restraint further rearward. With more reclined initial seatback angles the backset and torso to seatback distance increased. During impact, there was an increase in time before contact between the torso to seatback and head to head restraint. It was concluded that this was due to the fixed angle relationship between the seatback and head restraint.

The concept seat was modelled next and went through several iterations during the design. The aim of the design was to develop a seat system that would maintain an optimised seatback and head restraint position through a range of seatback angles. Simulations showed that this configuration was effective in minimising backset prior to and during a rear impact. The final design allowed for the concept seat to be set up as a standard seat by for comparative testing. This idea was carried through to the final seat design.

Note: Details of the model development have been omitted due to intellectual property conditions.

3.4 SIMULATION CONDITIONS

A 50th percentile male THOR dummy model was used in all MADYMO simulations. Data from sled tests with a THOR dummy in a rigid seat were previously used to validate the THOR model in rear impact at sled pulses ranging from 3 to 7g (Yuen et al. 2003).

MADYMO models require acceleration versus time histories to simulate the forces experienced during a collision. Firstly, a constant acceleration pointing vertically down was applied to the models to simulate acceleration due to gravity. Secondly, sled acceleration data was obtained from sled calibration runs. This data was formatted and inserted into MADYMO input files.

Two crash severity levels were used to simulate rear impact collisions. A 7g pulse (See Figure 3.2) was used to simulate a case where injury is likely to occur. A lower 3g pulse (See Figure 3.2) was used to simulate a case where injury is unlikely to occur.

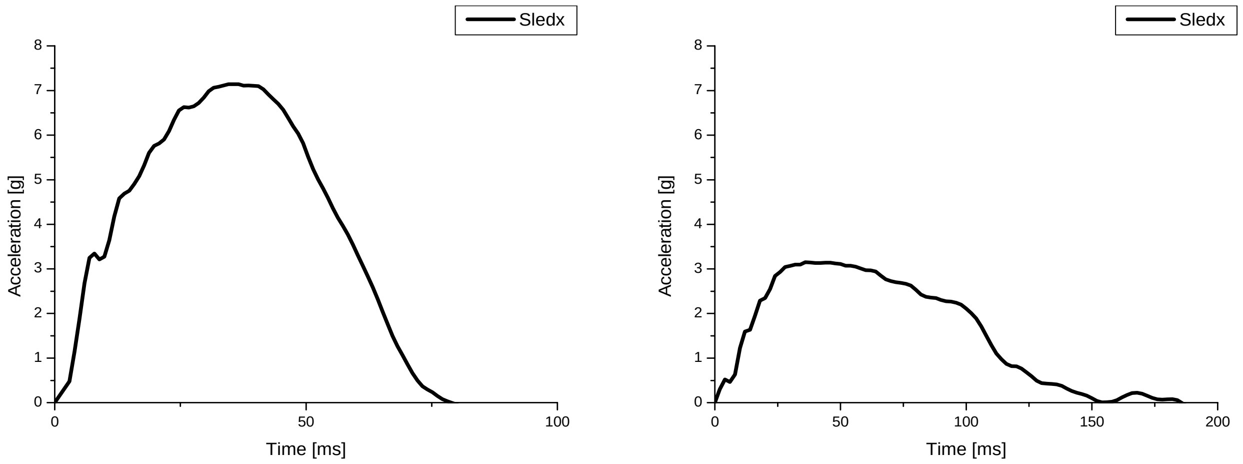

Figure 3.2: Acceleration versus time curves used to run MADYMO simulations. The plot on the left has a 7g peak acceleration and 80ms pulse width. The case on the right is a 3g peak acceleration and 150ms pulse width. The curves were obtained from sled calibration data.

3.5 DATA PROCESSING

All MADYMO model input files were created using a text editor. The models were then run in a Unix environment on a Dec-Alpha workstation. Output from each MADYMO simulation was processed using MATLAB. Several scripts were written to process the time history files and generate plots.

Custom routines were used to transfer the linear acceleration output file to MATLAB. Custom scripts then found and plotted the maximum accelerations of the head and T1. An indexing function was then used to determine the corresponding time of these maximum values. This data was then used to calculate and plot NIC values as a function of time. The routine was also used to load the relative displacement output file. Coordinates from this file were then used to calculate the T1 (α), link 1 (β) and link 2 (γ) angles relative to the sled (See Figure 3.3). These angles were then used to calculate the actual change of head (φ) and neck (θ) angles. These angles correspond to the two-link head and neck model used by Davidsson et al. (1999) to describe BioRID neck and head kinematics.

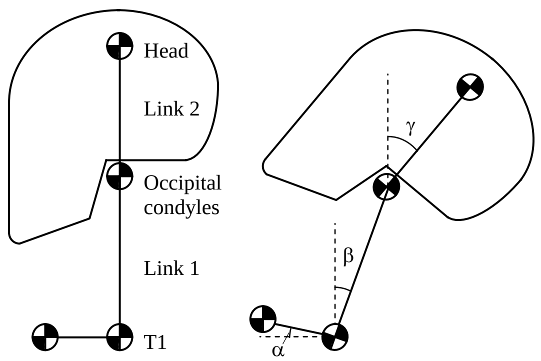

T1 angle: α

Link 1 angle: β

Link 2 angle: γ

Neck angle: $\theta = \beta - \alpha$

Head angle: $\varphi = \gamma - \beta - \alpha$

Figure 3.3: Two pivot neck link model describing Link 1 (β) and Link 2 (γ) angles relative to the sled and actual change in neck (θ) and head (φ) angles.

Run Name	Seat Configuration	Seatback Angle (deg)	Sled Pulse (g)	Backset (mm)
std15	Standard	15	7	70
std25	Standard	25	7	140
cs15	Concept	15	7	40
cs25	Concept	25	7	40

Table 3.1: Test matrix for 7g MADYMO simulations of standard (std) and concept (cs) seat configurations. The run name is the seat configuration followed by the seatback angle.

3.6 RESULTS

This section contains results for a series of 7g MADYMO simulations. The concept seat model was designed to allow for two different configurations. The standard seat (std) models a production seat with a fixed head restraint. The concept seat (cs) incorporates the new seat design. Each seat model was run with a 15 degree seat back angle and again with a 25 degree angle.

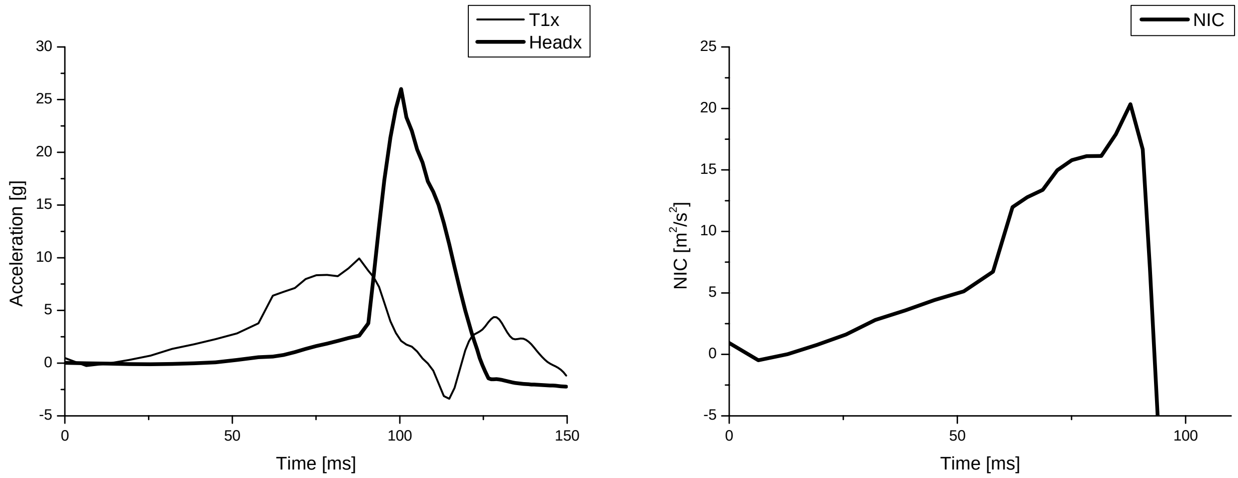

Figure 3.4: Test std15. Acceleration and NIC results for 7g MADYMO standard seat 15 degree test.

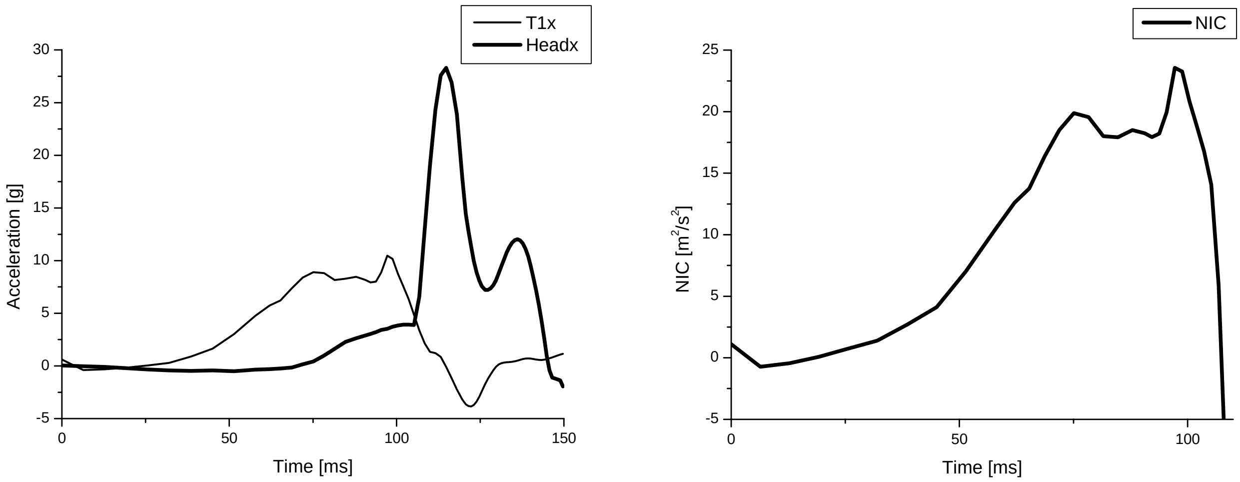

Figure 3.5: Test std25. Acceleration and NIC results for 7g MADYMO standard seat 25 degree test.

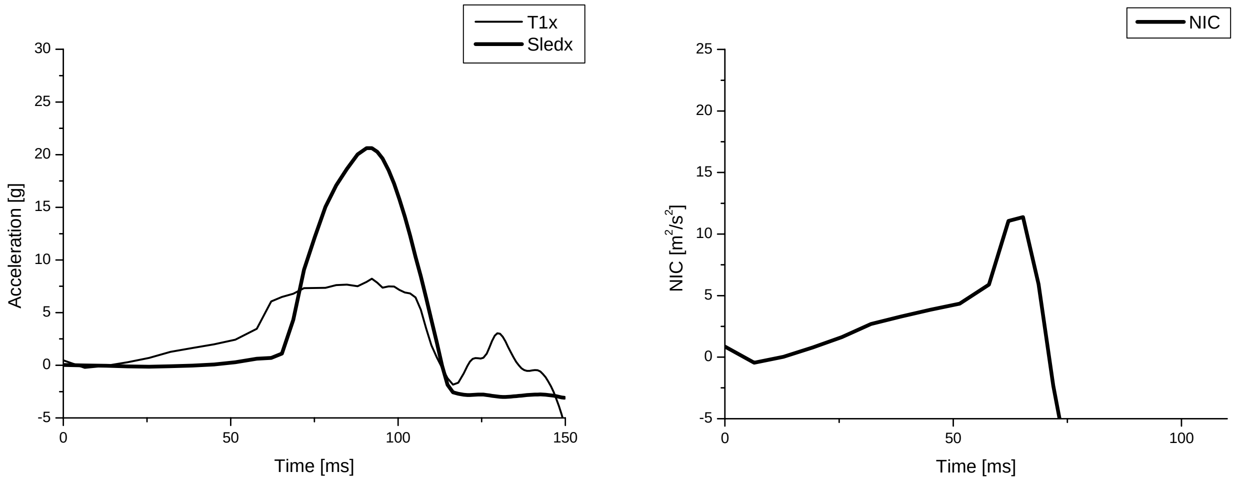

Figure 3.6: Test cs15. Acceleration and NIC results for 7g MADYMO concept seat 15 degree test.

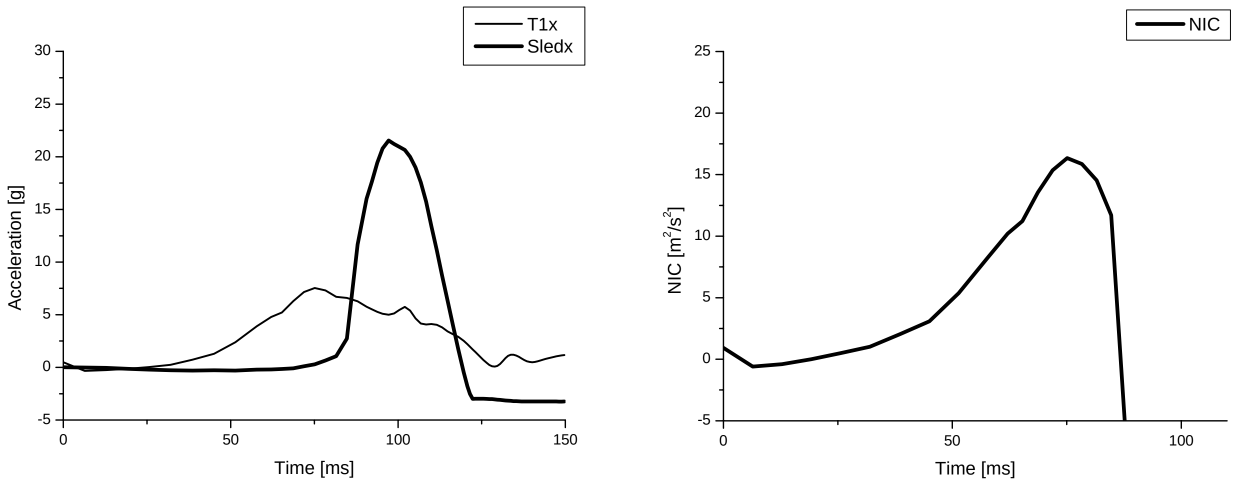

Figure 3.7: Test cs25. Acceleration and NIC results for 7g MADYMO concept seat 25 degree test.

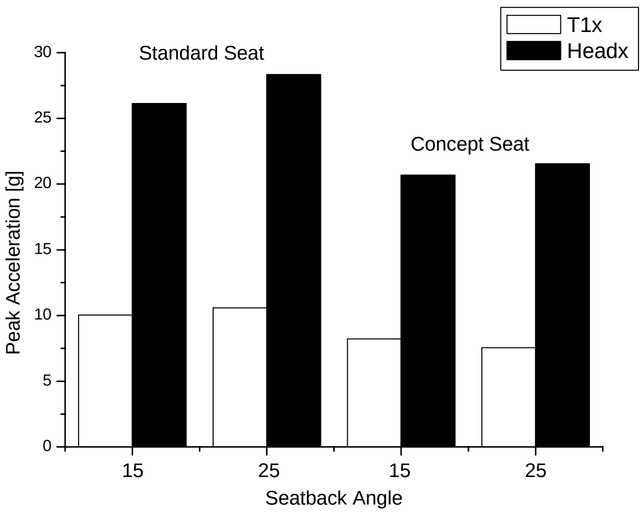

Figure 3.8: Maximum x-acceleration of the head and T1 for each MADYMO model seat configuration. The concept seat head accelerations are significantly lower than the standard seat head accelerations while the T1 values are slightly lower.

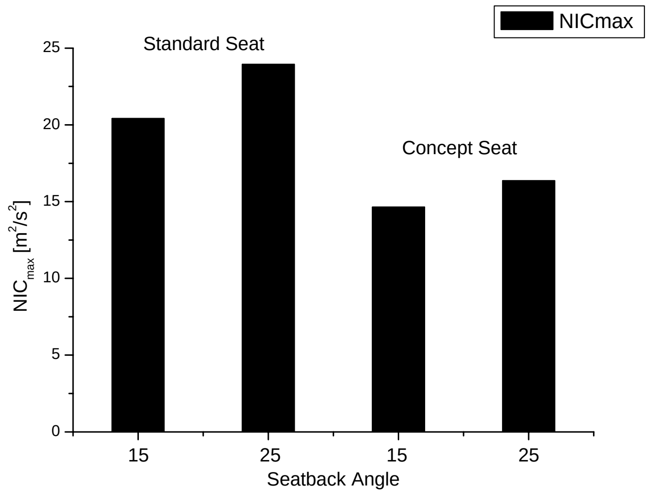

Figure 3.9: Maximum NIC value for each MADYMO model seat configuration. The concept seat NIC values are significantly lower than the standard seat NIC values.

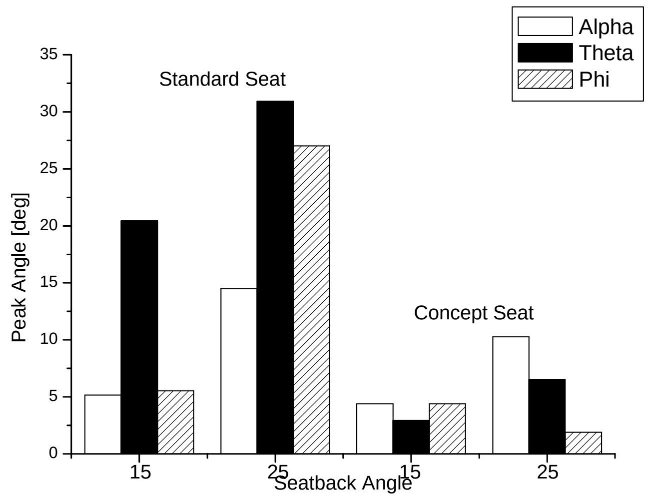

Figure 3.10: The maximum head (φ), neck (θ) and T1 (α) angles for each MADYMO model seat configuration. The concept seat angles are lower than the standard seat angles. See Figure 3.3 for angle definitions.

3.7 DISCUSSION

There are three main results to discuss with the MADYMO simulation: Maximum acceleration of the head and T1, the maximum NIC values and finally the head, neck and T1 angles.

The acceleration for head and T1 have been plotted against time for tests std15, std25, cs15 and cs25 in Figure 3.4 through to Figure 3.7 respectively. The maximum values have been summarised in a bar graph (See Figure 3.8). For the standard seat the head acceleration for the 15 degree case is 2.25g less than the 25 degree case. Similarly, the T1 acceleration for the 15 degree case is 0.61g less than the 25 degree case. The 25 degree case has a larger initial backset and hence the head has more time to translate and rotate in extension hence the higher peak head acceleration. The T1 acceleration follows the same explanation with more torso displacement due to a larger initial torso to seat back distance. For the concept seat the head acceleration for the 15 degree case is 0.87g less than the 25 degree case. However, the T1 acceleration for the 15 degree case is 0.66g more than the 25 degree case. Both peak accelerations are similar in magnitude and this can be explained by the head restraint maintaining a minimised backset at all times. The T1 accelerations are also similar and this is due to the new seatback design that keeps the upper seat back close to the dummy torso at all times. Head and T1 accelerations for the concept seat were lower than the accelerations for the standard seat.

NIC values have been plotted against time for tests std15, std25, cs15 and cs25 in Figure 3.4 through to Figure 3.7 respectively. The maximum values have been summarised in a bar graph (See Figure 3.9). For the standard seat the NIC for the 15 degree case is $3.5 m^2/s^2$ less than the 25 degree case. For the concept seat the NIC for the 15 degree case is $1.7 m^2/s^2$ less than the 25 degree case. The NIC values for the concept seat were lower than the NIC values for the standard seat. While the peak accelerations contribute to the NIC values, it is also important to note the time difference between the start of the head acceleration when compared to the start of the T1 acceleration. The relative acceleration of the NIC equation (See Equations 1-3) is the difference between the T1 and head acceleration. For the standard seat cases the head acceleration (See Figure 3.4 and 3.5) commences during the T1 pulse and continues after the T1 pulse has returned to zero. For the concept seat cases the head and T1 acceleration pulses (See Figures 3.6-3.7) occur within the same range of time. The result is a more uniform acceleration of the head and torso and hence lower NIC values for the concept seat. This result is due primarily to the minimised backset as well as the minimised torso to seat back distance.

The head (φ), neck (θ) and T1 (α) (See Figure 3.3) have been plotted for tests std15, std25, cs15 and cs25 in a summary bar graph (See Figure 3.10). While the individual angles are important, the crucial angles to look at are theta and phi which represent the change in neck angle and change in head angle respectively. For the standard seat theta for the 15 degree case is 1.9 degrees less than the 25 degree case. Phi for the 15 degree case is 21.5 degrees less than the 25 degree case. This is a significant amount of head rotation when compared to the 15 degree case. For the concept seat theta for the 15 degree case is 1 degree less than the 25 degree case. Phi for the 15 degree case is 2.5 degrees more than the 25 degree case. All angles for the concept seat were significantly lower than the angles for the standard seat. While there was a slight increase between the 15 and 25 degree concept seat, the difference between the 15 and 25 degree standard seat is more significant.

Overall, the results showed a good correlation between the maximum acceleration of the head and T1, the maximum NIC values and the head, neck and T1 angles. In all standard seat cases the 25 degree case performed worse than the 15 degree case. This was due to the increased backset associated with the increased initial seatback angle and fixed head restraint. It was also observed that the torso loads the seatback and causes it to rotate rearward. Since the head restraint is fixed relative to the seatback, the head restraint moves further away and increases backset.

In all concept seat cases both the 15 degree and 25 degree results were similar. These results show that the concept seat not only reduces overall injury potential, but does so irrespective of initial seat back angle. The seat also proved to minimise the backset through out the rear impact simulation.

CHAPTER 4 - DETAIL DESIGN AND MANUFACTURING OF PROTOTYPE 1

4.1 PROTOTYPE DETAIL DESIGN

The initial idea was to obtain two identical standard production seats. One seat would be modified into a concept seat and the remaining seat would be used as the benchmark. By basing the concept seat on production seat geometry, it would be possible to make a sensible comparison between the two seats in terms of anti-whiplash performance.

As the design evolved, it was determined that it would be possible to combine both the standard seat and concept seat configurations into a single seat. The concept seat system was designed to be a removable sub-assembly. It was therefore possible to revert the concept seat back to a typical standard seat for comparison purposes.

Geometry from the MADYMO concept seat models was used to create 3D CAD components that were then used to assemble a 3D model (See Figure 4.1). Engineering drawings were generated from the 3D models to be used during the manufacturing process.

To ensure the suitability of materials chosen for construction, engineering analysis was performed on critical areas of the design. Maximum loads were determined through the expected peak accelerations and the mass of the dummy. A worst case scenario of the entire dummy mass loading one side of the seat frame was assumed. This was coupled with a factor of safety to ensure a safe threshold. Beam bending calculations were performed for the frame and shear pin calculations were performed for all fastener locations.

Note: Details of the manufacturing process have been omitted due to intellectual property conditions.

CHAPTER 5 - SLED TESTING OF PROTOTYPE 1

5.1 INTRODUCTION

Rear impact sled testing of the concept seat with a seated THOR dummy was conducted to verify the design. The intention was to run a series of tests with the seat in both standard and concept configuration and compare how each seat influences the dummies motion.

5.2 METHODS

Rear impact crash testing of the concept seat was conducted on a custom designed rebound crash sled at the Prince of Wales Medical Research Institute. The sled was calibrated for a change in velocity (Δv) of 12.5kph and peak acceleration of 70m/s^2 (7.1g).

The concept seat was rigidly mounted to the sled via a custom built frame. The seat was set to align the seatback centreline at both 15 and 25 degrees from the vertical. A THOR dummy was positioned with an upright driving posture using an inbuilt tilt sensor system. A lap belt was used to restrain the dummy's abdomen and both feet were secured to the footrest with webbing. This was only a precaution to protect the dummy from potentially falling out of the seat on the rebound phase.

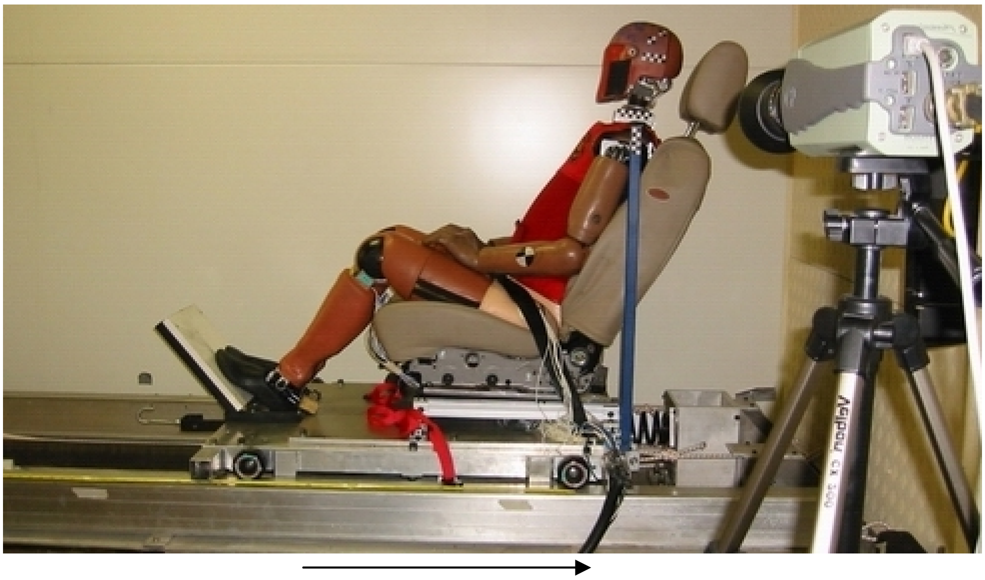

Direction of inbound travel

Figure 5.1: Sled configured for a low-speed rear impact simulation with a THOR dummy. The sled travels from left to right and rebounds off the spring barrier. The high-speed camera in the foreground is used to record each test for optical marker analysis.

Tri-axial accelerometer blocks were used to attach Entran EGE 750g accelerometers to the head centre of gravity and T1. An additional accelerometer was attached to the sled to measure the x acceleration. An Applied Measurement signal conditioner was used to acquire data at 10 kHz in accordance with SAE J211/1 standards. A Phantom high-speed camera recording at 500 frames per second was used to record each test for marker analysis and visual inspection. The camera and data acquisition are both triggered by an optical switch on the side of the sled. The optical switch set-up doubles as a time trap to measure impact and rebound velocity.

Optical markers were applied to several key locations including the head centreline, head centre of gravity, the occipital condyles, T1 via a custom made bracket and the sled (See Figure 5.2). The high-speed video was processed to generate single images at 2ms intervals. Code was written in MATLAB to track the optical marker locations. The coordinates where then used to calculate the T1 (α), link 1 (β) and link 2 (γ) angles relative to the sled (See Figure 3.3). These angles were then used to calculate the actual change of neck (θ) and head (φ) angles. This procedure was based on techniques developed during the MADYMO modelling study (See 3.5 Methods).

Figure 5.2: A THOR dummy in the standard seat configuration (left) and the concept seat configuration (right). Note how the concept seat conforms to the dummy and minimizes the initial backset.

Run Name	Seat Configuration	Seatback Angle (deg)	Sled Pulse (g)	Backset (mm)
std15	Standard	15	7	80
std25	Standard	25	7	120
cs15	Concept	15	7	10
cs25	Concept	25	7	10

Table 5.1: Test matrix for 7g sled tests for standard (std) and concept (cs) seat configurations. The run name is the seat configuration followed by the seatback angle. This matrix was chosen to evaluate the standard and concept seat both with a standard and active head restraint. Two angles were chosen to show that as seatback angle increases, the standard seat safety decreases while the concept seat safety remains constant.

5.3 RESULTS

This section contains results for a series of 7g sled tests. The standard seat (std) is a production seat with a fixed head restraint. The concept seat (cs) incorporates a new seatback design. Each seat configuration was tested with a 15 degree seat back angle and again with a 25 degree angle.

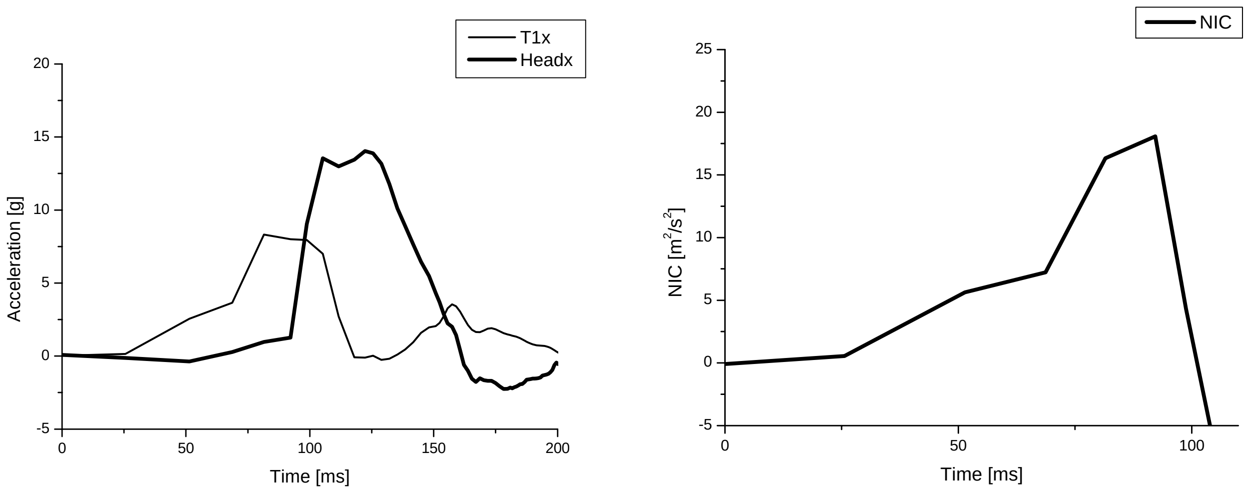

Figure 5.3: Test std15. Acceleration and NIC results for 7g Prototype 1 standard seat 15 degree test.

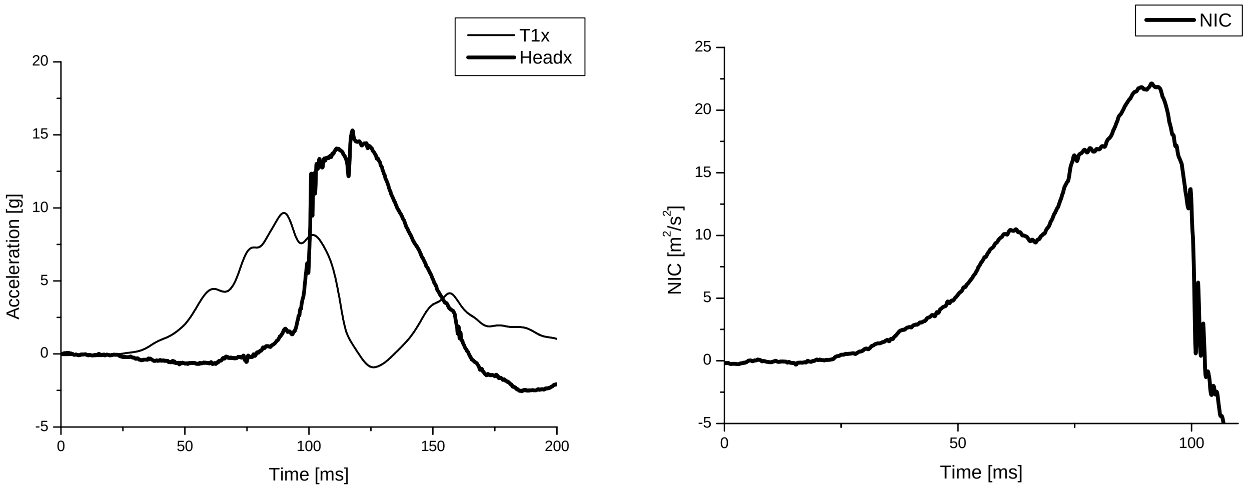

Figure 5.4: Test std25. Acceleration and NIC results for 7g Prototype 1 standard seat 25 degree test.

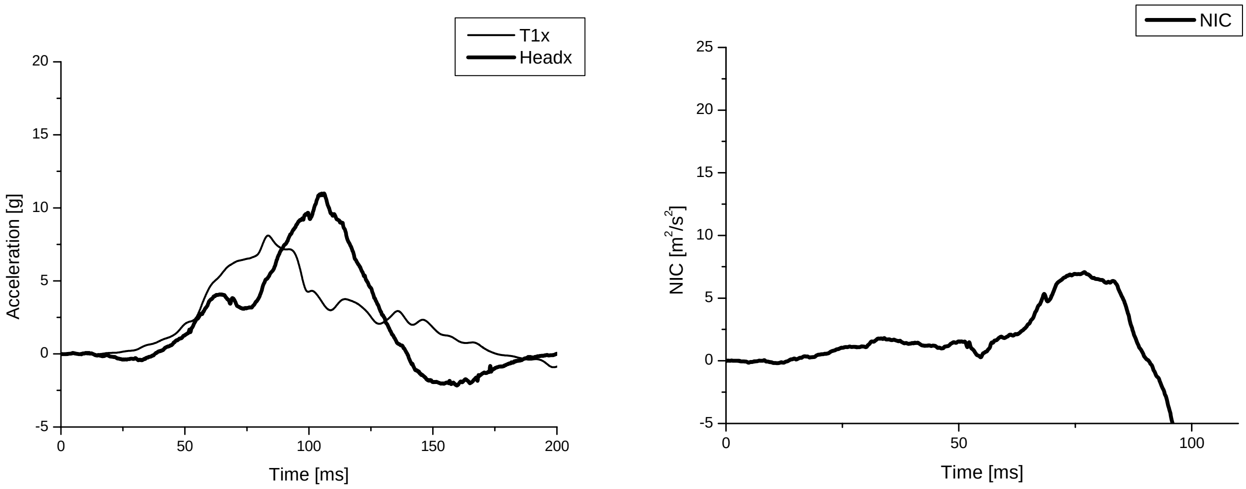

Figure 5.5: Test cs15. Acceleration and NIC results for 7g Prototype 1 concept seat 15 degree test.

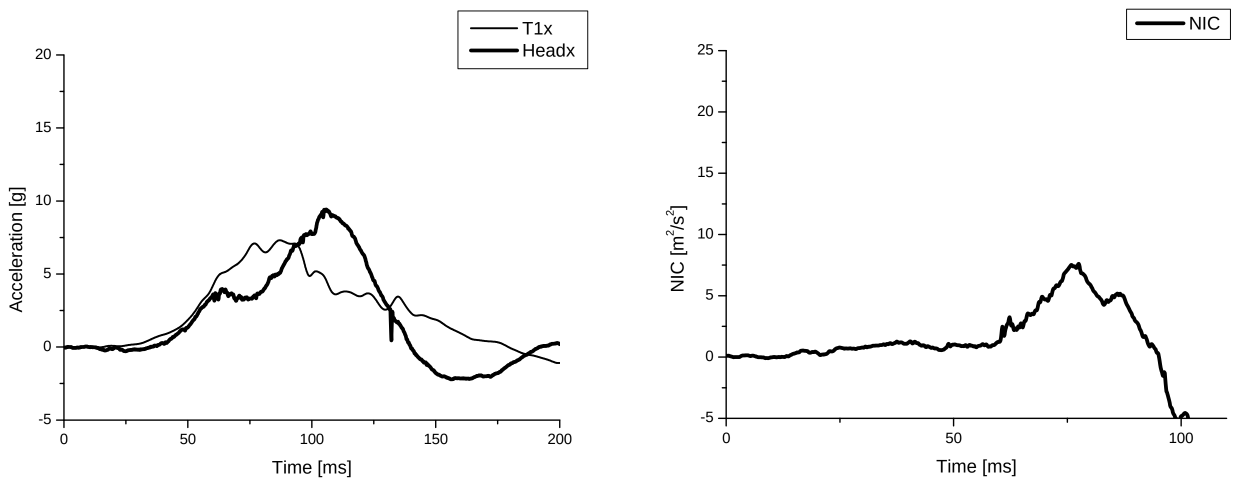

Figure 5.6: Test cs25. Acceleration and NIC results for 7g Prototype 1 concept seat 25 degree test.

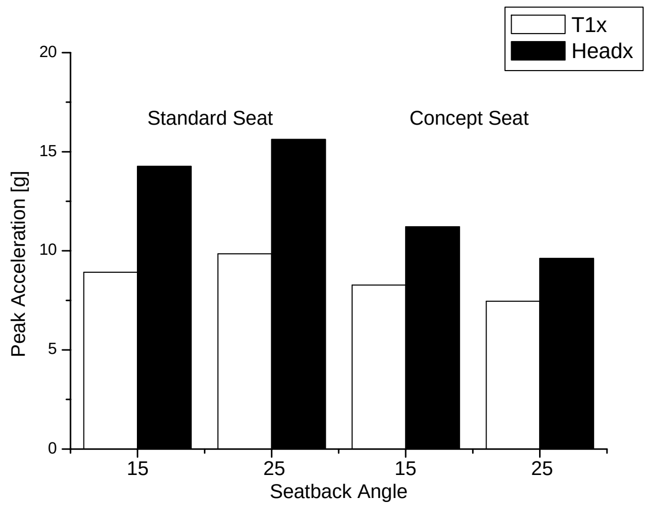

Figure 5.7: Maximum x-acceleration of the head and T1 for each Prototype 1 seat configuration. The concept seat head accelerations are significantly lower than the standard seat head accelerations while the T1 values are slightly lower.

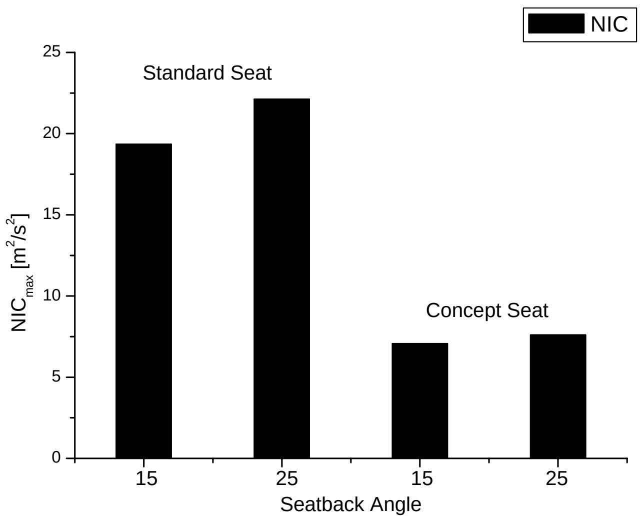

Figure 5.8: Maximum NIC value for each Prototype 1 seat configuration. The concept seat NIC values are significantly lower than the standard seat NIC values.

5.4 DISCUSSION

There are two main results to discuss with the Prototype 1 tests: Maximum acceleration of the head and T1 and the maximum NIC values.

The accelerations for head and T1 have been plotted against time for tests std15, std25, cs15 and cs25 in Figure 5.3 through to Figure 5.6 respectively. The maximum values have been summarised in a bar graph (See Figure 5.7). For the standard seat the head acceleration for the 15 degree case is 5.34g less than the 25 degree case. The T1 acceleration for the 15 degree case is 0.93g less than the 25 degree case. The 25 degree case has a larger initial backset and hence the head has more time to translate and rotate in extension hence the higher peak head acceleration. The T1 acceleration follows the same explanation with more torso displacement due to a larger initial torso to seat back distance. For the concept seat the head acceleration for the 15 degree case is 2.95g less than the 25 degree case. However, the T1 acceleration for the 15 degree case is 0.81g more than the 25 degree case. Both peak accelerations are similar in magnitude and this can be explained by the head restraint maintaining a minimised backset at all times. The T1 accelerations are also similar and this is due to the new seatback design that keeps the upper seatback close to the dummy torso at all times. Head and T1 accelerations for the concept seat were lower than the accelerations for the standard seat.

NIC values have been plotted against time for tests std15, std25, cs15 and cs25 in Figure 5.3 through to Figure 5.6 respectively. The maximum values have been summarised in a bar graph (See Figure 5.8). For the standard seat the NIC for the 15 degree case is $2.78m^2/s^2$ less than the 25 degree case. For the concept seat the NIC for the 15 degree case is $0.54m^2/s^2$ less than the 25 degree case. The NIC values for the concept seat were significantly lower than the NIC values for the standard seat (See Figure 5.8). While the peak accelerations contribute to the NIC values, it is also important to compare the time difference between the start of both the head and T1 acceleration. The relative acceleration of the NIC equation (See Equations 1-3) is the difference between the T1 and head acceleration.

For the standard seat cases the head acceleration (See Figure 5.3 and 5.4) commences during the T1 pulse and continues after the T1 pulse has returned to zero. For the concept seat cases the head and T1 acceleration pulses (See Figures 5.5-5.6) occur within the same range of time. The result is a more uniform acceleration of the head and torso and hence lower NIC values for the concept seat. This result is due primarily to the minimised backset as well as the minimised torso to seat back distance.

Overall, the results showed a good correlation between the maximum acceleration of the head and T1 and the maximum NIC values. In all standard seat tests the 25 degree case performed worse than the 15 degree case. This was due to the increased backset associated with the increased seatback angle and fixed head restraint as well as the torso pushing the seatback, and in turn head restraint, further away from the head. It was observed that during a rear impact, the torso would load the seat back and cause an increase in seatback angle and hence force the head restraint to move away from the rear of the head causing an increased back set.

In all concept seat cases both the 15 degree and 25 degree results were similar. These results show that the concept seat not only reduces overall injury potential, but does so irrespective of initial seat back angle. The effectiveness of the new seatback design in the concept seat was evident in the minimised backset through out the rear impact simulation.

When compared to the 15 degree standard seat, the use of the new seatback design reduces the NIC value by 63.5%. Similarly for the 25 degree standard seat where the use the new seatback reduces the NIC value by 65.6%. These results clearly show the whiplash reduction potential of the new seatback design.

The main limitation of this design is that the head restraint was positioned too close to the dummy head. A design improvement would be to position the head restraint slightly further away from the head. At the same time, it would be interesting to see if incorporating an active head restraint would help reduce this backset during a rear impact.

CHAPTER 6 - DESIGN IMPROVEMENTS FOR PROTOTYPE 2

6.1 HEAD RESTRAINT GEOMETRY

The head restraint on Prototype 1 was positioned too close to the dummy head for the concept seat configurations with an initial backset of 10mm. The results were minimised accelerations and NIC values, however the backset was deemed impractical for production seats since the proximity of the head restraint could induce occupant discomfort. Consequently, the head restraint mounting plates were redesigned to allow for a more realistic head restraint position with an initial backset of 40mm for the concept seat.

6.2 ACTIVE HEAD RESTRAINT

With this increased backset for the concept seat configuration, it was decided that it would be of interest to evaluate whether an active head restraint would contribute to reducing the amount of head and neck motion and hence injury risk. A design based on the SAHR concept (See Section 1.1.3) was thus incorporated.

A plate attached to a steel mesh frame was incorporated into the seat back that could be loaded by the torso during a rear impact. Through a lever mechanism, the rearward translation of the plate moves the head restraint upward and forward. Since the active head restraint mechanism was to be incorporated into the existing concept seat, it was important to design the mechanism around the new seatback design. Initially there were concerns about how changing seat back angles would affect the initial head restraint position. This was solved by locating the upper hinge of the active head restraint mesh in a suitable location.

To be able to compare the difference between both standard seat and concept seat with and without an active head restraint, a pair of lock pins was added to the design. When installed, these extra pins rigidly lock the active head restraint mechanism.

Note: Details of the design improvements have been omitted due to intellectual property conditions.

CHAPTER 7 - SLED TESTING OF PROTOTYPE 2 WITH A THOR DUMMY

7.1 INTRODUCTION

Rear impact sled testing of the concept seat with a seated THOR dummy was conducted to verify the design. The intention was to run a series of tests with the seat in both standard and concept configuration and compare how each seat influences the dummies motion.

7.2 METHODS

The procedure for Prototype 1 testing was repeated for Prototype 2 testing (See Chapter 5).

Run Name	Seat Configuration	Seatback Angle (deg)	Head Restraint	Sled Pulse (g)	Backset (mm)
std15std	Standard	15	Standard	7	80
std15act	Standard	15	Active	7	80
std25std	Standard	25	Standard	7	120
std25act	Standard	25	Active	7	120
cs15std	Concept	15	Standard	7	40
cs15act	Concept	15	Active	7	40
cs25std	Concept	25	Standard	7	40
cs25act	Concept	25	Active	7	40

Table 7.1: Test matrix for 7g sled tests for standard and concept seat configurations with a standard and active head restraint. The run name is the seat configuration followed by the seatback angle and finally the head restraint configuration. This matrix was chosen to thoroughly evaluate the standard and concept seat both with a standard and active head restraint. Two angles were chosen to show that as seatback angle increases, the standard seat safety decreases while the concept seat safety remains constant.

7.3 RESULTS

This section contains results for a series of 7g sled tests. Both the standard seat (std) and concept seat (cs) were tested with a standard (std) as well as an active (act) head restraint. Each seat configuration was tested with a 15 degree seat back angle and again with a 25 degree angle.

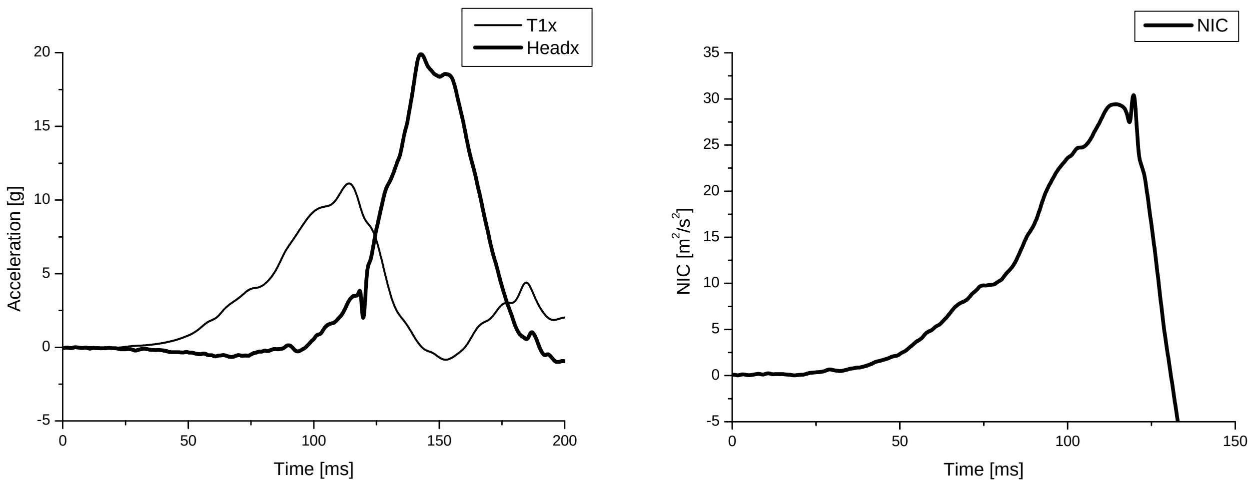

Figure 7.1: Test std15std. Acceleration and NIC results for 7g Prototype 2 standard seat 15 degree test with standard head restraint.

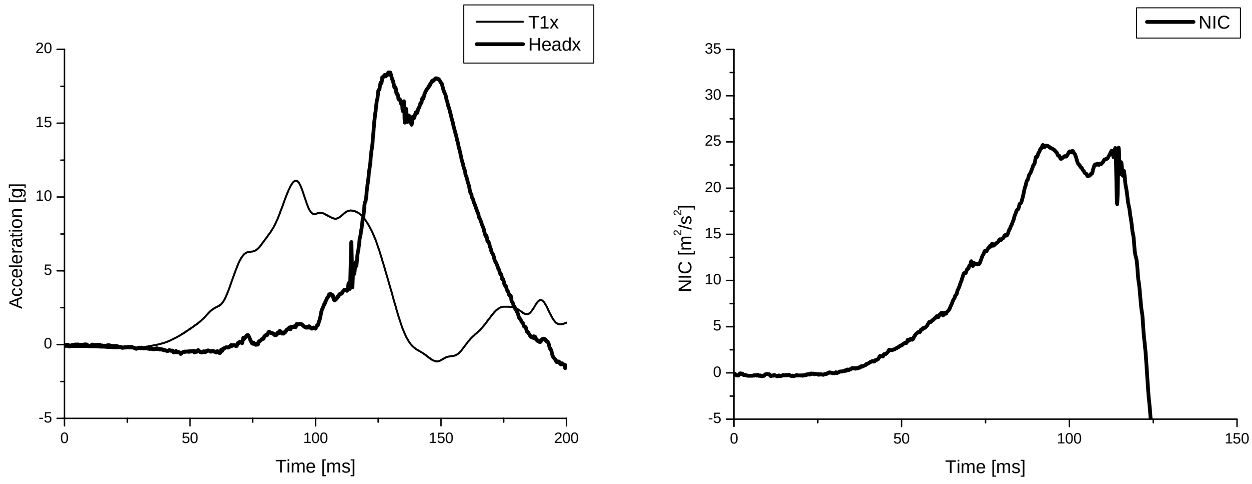

Figure 7.2: Test std15act. Acceleration and NIC results for 7g Prototype 2 standard seat 15 degree test with standard head restraint.

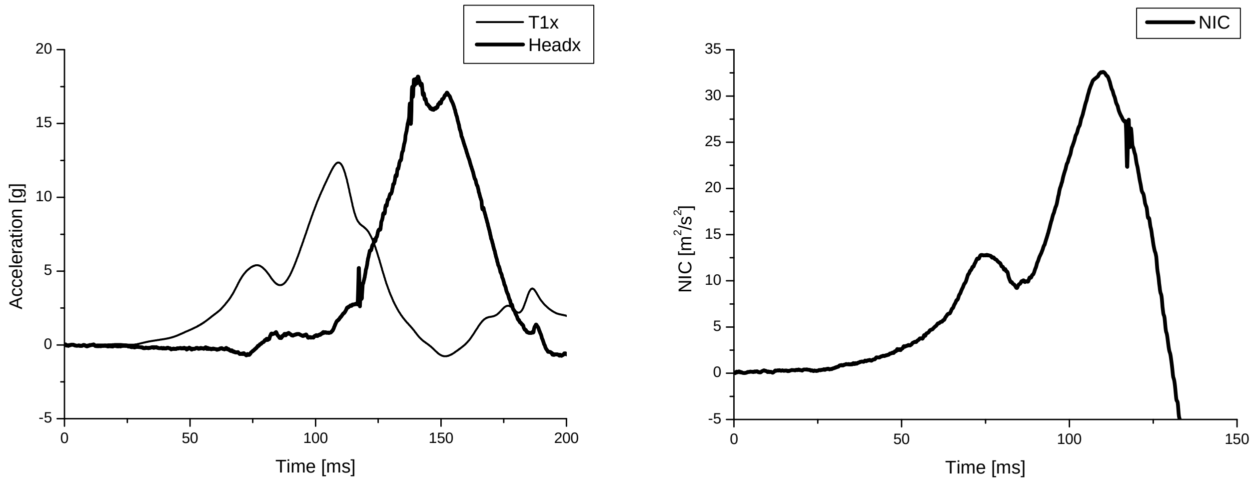

Figure 7.3: Test std25std. Acceleration and NIC results for 7g Prototype 2 standard seat 25 degree test with standard head restraint.

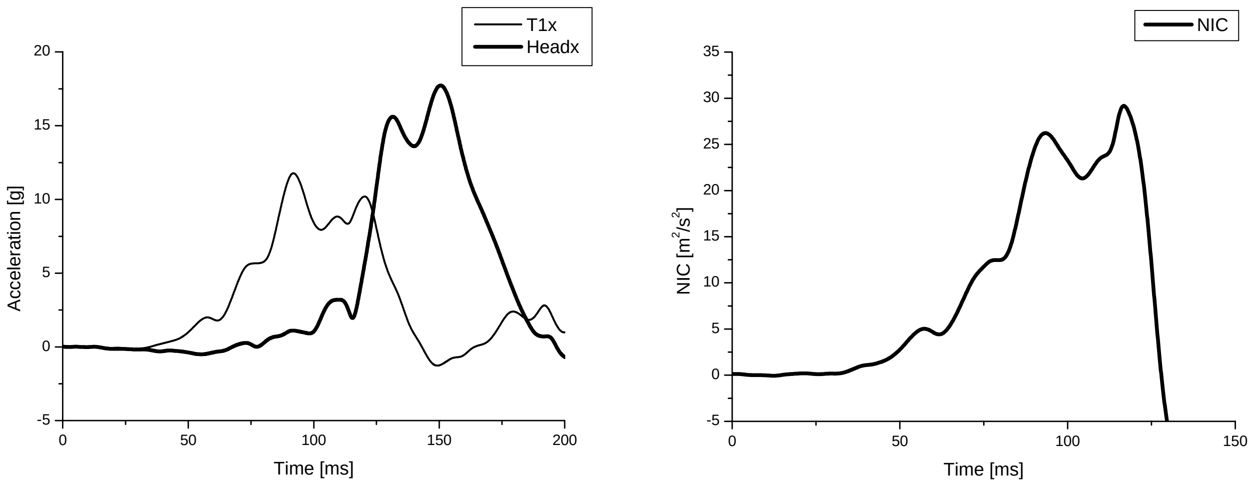

Figure 7.4: Test std25act. Acceleration and NIC results for 7g Prototype 2 standard seat 25 degree test with standard head restraint.

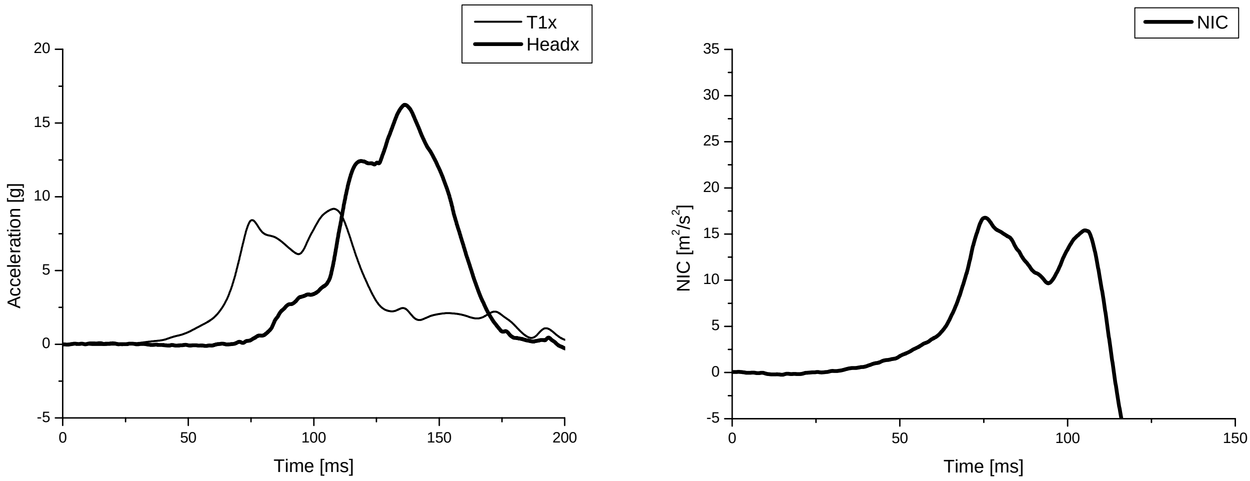

Figure 7.5: Test cs15std. Acceleration and NIC results for 7g Prototype 2 concept seat 15 degree test with standard head restraint.

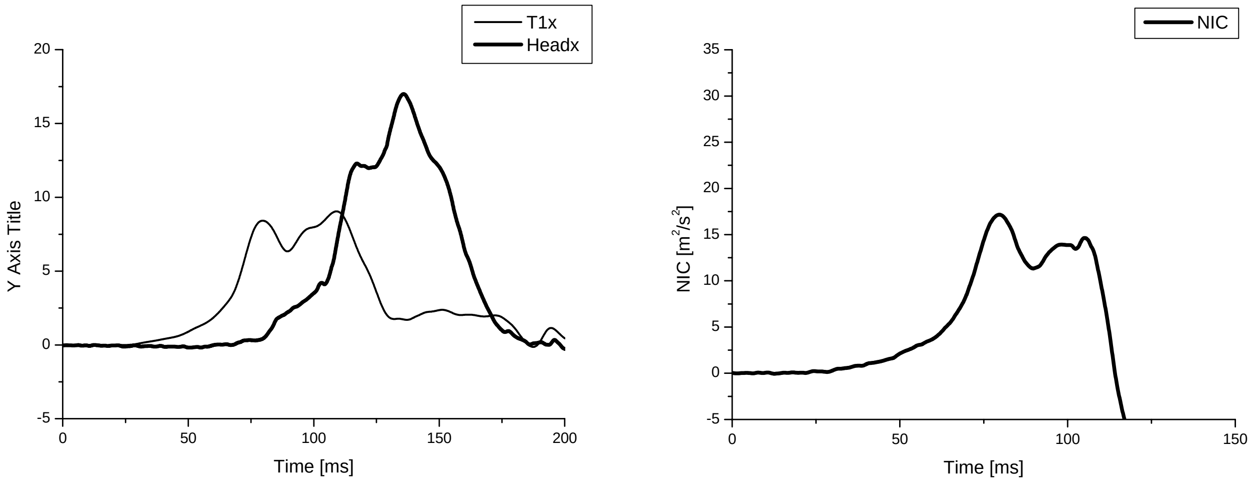

Figure 7.6: Test cs15act. Acceleration and NIC results for 7g Prototype 2 concept seat 15 degree test with active head restraint.

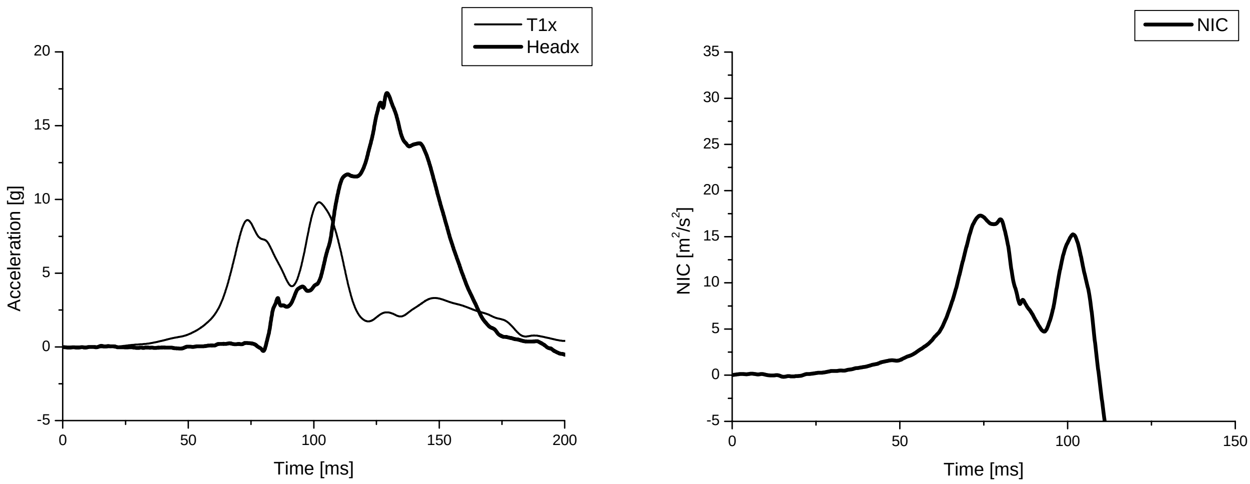

Figure 7.7: Test cs25std. Acceleration and NIC results for 7g Prototype 2 concept seat 25 degree test with standard head restraint.

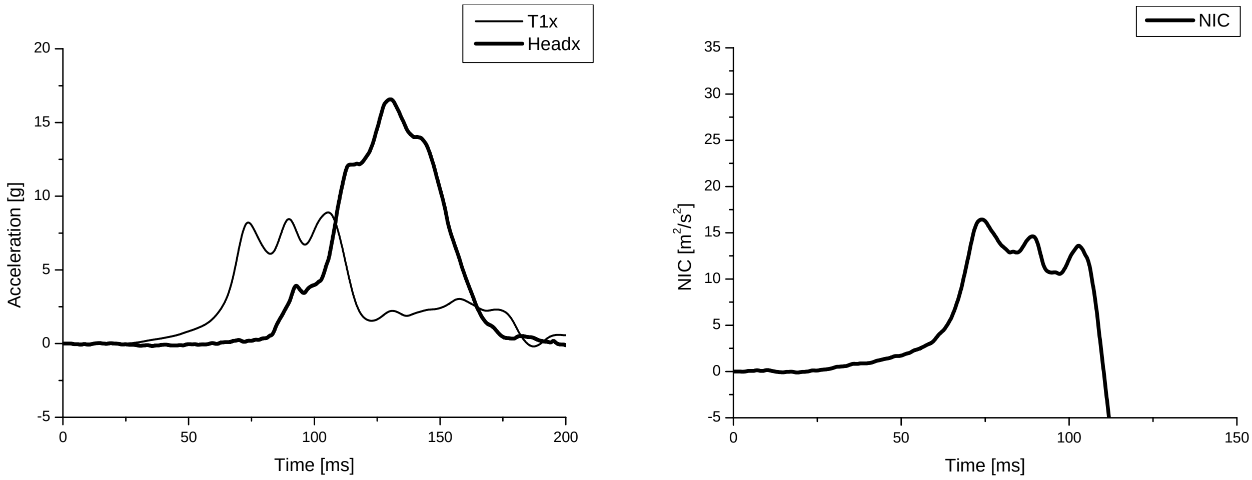

Figure 7.8: Test cs25act. Acceleration and NIC results for 7g Prototype 2 concept seat 25 degree test with active head restraint.

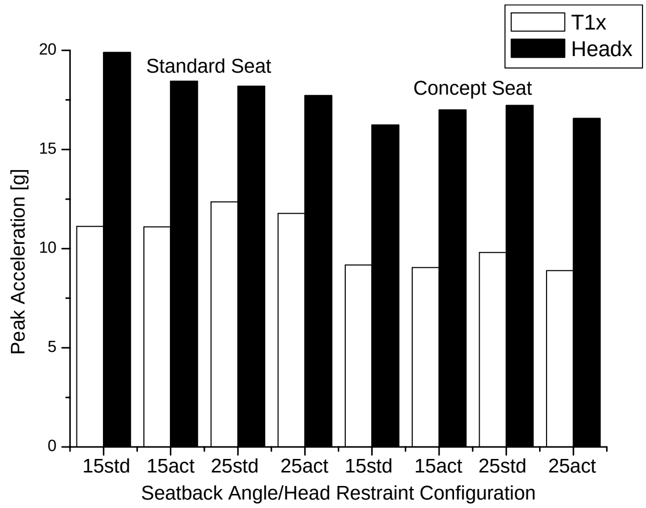

Figure 7.9: Maximum x-acceleration of the head and T1 for each Prototype 2 seat configuration. The concept seat head and T1 accelerations are lower than the standard seat head accelerations.

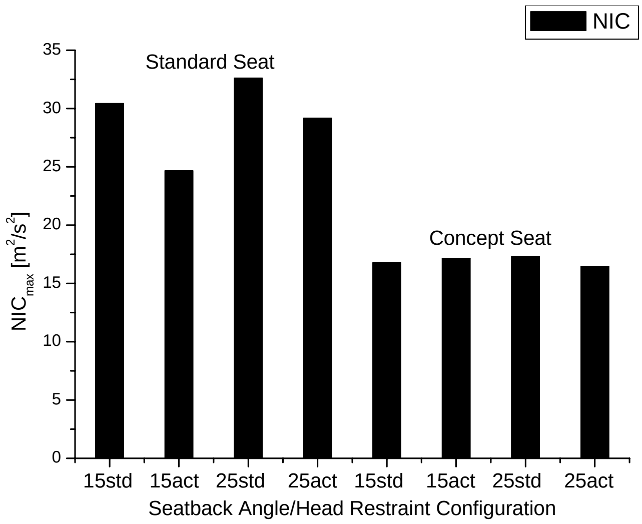

Figure 7.10: Maximum NIC value for each Prototype 2 seat configuration. The concept seat NIC values are lower than the standard seat NIC values. The NIC values are lower for tests with the active head restraint when compared to tests with a standard head restraint. NIC values increase for the standard seat as seat back angle increases while the NIC values for the concept seat remain constant as the seat back angle increases.

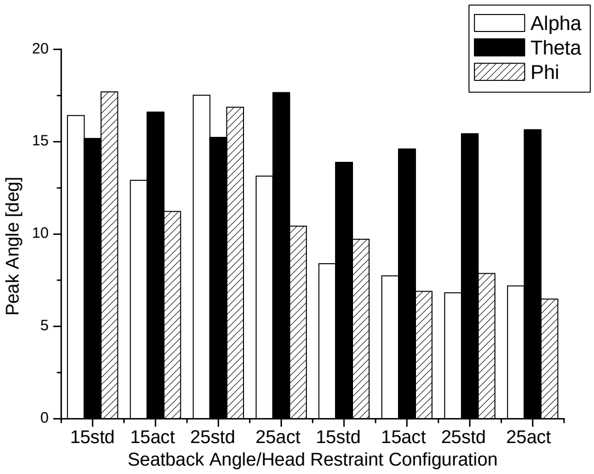

Figure 7.11: The maximum head (φ), neck (θ) and T1 (α) angles for each Prototype 1 seat configuration. Overall, the concept seat angles are lower than the standard seat angles. See Figure 3.3 for angle definitions.

7.4 DISCUSSION

There are three main results to discuss with the Prototype 2 tests: Peak acceleration of the head and T1, maximum NIC values and the maximum head, neck and T1 angles.

The accelerations for head and T1 have been plotted against time for tests std15std, std15act, std25std, std25act, cs15std, cs15act, cs25std and cs25act in Figure 7.1 through to Figure 7.8 respectively. The maximum values have been summarised in a bar graph (See Figure 7.9). For the standard seat with a fixed head restraint the head acceleration for the 15 degree case is 1.46g more than the 25 degree case. The T1 acceleration for the 15 degree case is 1.24g less than the 25 degree case. The 25 degree case has a larger initial backset and hence the head has more time to translate and rotate in extension hence the higher peak head acceleration. The T1 acceleration follows the same explanation with more torso displacement due to a larger initial torso to seat back distance. When the active head restraint was used, a reduction in peak accelerations for both head and T1 were seen. For the concept seat with a fixed head restraint the head acceleration for the 15 degree case is 0.98g less than the 25 degree case. Similarly, the T1 acceleration for the 15 degree case is 0.63g less than the 25 degree case. Both peak accelerations are similar in magnitude and this can be explained by the head restraint maintaining a minimised backset at all times. The T1 accelerations are also similar and this is due to the new seatback design that keeps the upper seat back close to the dummy torso at all times. When the active head restraint was used, slight reductions in peak accelerations for both head and T1 were seen. Head and T1 accelerations for the concept seat were lower than the accelerations for the standard seat.

NIC values have been plotted against time for tests std15std, std15act, std25std, std25act, cs15std, cs15act, cs25std and cs25act in Figure 7.1 through to Figure 7.8 respectively. The maximum values have been summarised in a bar graph (See Figure 7.10). For the standard seat with a fixed head restraint the NIC for the 15 degree case is $2.91m^2/s^2$ less than the 25 degree case. When the active head restraint was used, the 15 degree case is $4.51m^2/s^2$ less than the 25 degree case. This shows that the standard seat benefits from the addition of an active head restraint. For the concept seat with a fixed head restraint the NIC for the 15 degree case is $0.52m^2/s^2$ less than the 25 degree case. When the active head restraint was used, the 15 degree case is $0.72m^2/s^2$ more than the 25 degree case. This shows that the concept seat does not significantly benefit from the addition of an active head restraint. The NIC values for the concept seat were significantly lower than the NIC values for the standard seat (See Figure 7.10). While the peak accelerations contribute to the NIC values, it is also important to compare the time difference between the start of both the head and T1 acceleration. The relative acceleration of the NIC equation (See Equations 1-3) is the difference between the T1 and head acceleration. For the standard seat cases the head acceleration (See Figure 7.1 and 7.4) commences during the T1 pulse and continues after the T1 pulse has returned to zero. For the concept seat cases the head and T1 acceleration pulses (See Figures 7.5-5.8) occur within the same range of time. The result is a more uniform acceleration of the head and torso and hence lower NIC values for the concept seat. This result is primarily due to the minimised backset as well as the minimised torso to seat back distance.

Peak angles for the head, neck and T1 have been plotted for tests std15std, std15act, std25std, std25act, cs15std, cs15act, cs25std and cs25act have been plotted in a bar graph (See Figure 7.11). Alpha, beta, theta, gamma and phi represent T1, link 1, neck, link 2 and head angle respectively (See Figure 3.3). For the standard seat with a fixed head restraint the peak angles for the 15 degree case are lower than the peak angles for the 25 degree case. When the active head restraint was used, peak angles for the 15 degree case are lower than the peak angles for the 25 degree case. Both cases with the active head restraint showed lower peak angles when compared to the fixed head restraint cases. This shows that the standard seat benefits from the addition of an active head restraint. For the concept seat with a fixed head restraint the peak angles for the 15 degree case are similar to the peak angles for the 25 degree case. Similarly when the active head restraint was used, the peak angles for the 15 degree case are similar to peak angles for the 25 degree case. This shows that the concept seat does not significantly benefit from the addition of an active head restraint.

The peak angles for the concept seat were significantly lower than the peak angles for the standard seat (See Figure 7.11). The lower peak angles are due to the minimised initial backset (See Table 7.1), which limits the amount of head, neck and T1 motion. In addition, when the torso loads the seatback the new seatback design maintains an upright upper seatback and optimal head restraint position.

Overall, the results showed a good correlation between the maximum acceleration of the head and T1, the maximum NIC values and peak head, neck and T1 angles. In all standard seat tests the 25 degree case performed worse than the 15 degree case. This was due to the increased backset associated with the increased seatback angle and fixed head restraint as well as the torso pushing the seatback, and in turn head restraint, further away from the head. It was observed that during a rear impact, the torso would load the seat back and cause an increase in seatback angle and hence force the head restraint to move away from the rear of the head causing an increased back set.

In all concept seat cases both the 15 degree and 25 degree results were similar. These results show that the concept seat not only reduces overall injury potential, but does so irrespective of initial seat back angle. The effectiveness of the new seatback design in the concept seat was evident in the minimised backset through out the rear impact simulation.

For a 15 degree standard seat with a fixed head restraint the NIC value was reduced by 18.88% when an active head restraint was implemented. The new seatback design with a fixed head restraint reduces the NIC value by 44%. Similarly for the 25 degree standard seat with a fixed head restraint where the use of an active head restraint reduces the NIC value by 10.5% while the new seatback design reduces the NIC value by 47%. These results clearly show the whiplash reduction potential of the new seatback design.

The main limitation of this test series was the use of the THOR dummy. Initially proposed as an omni-directional dummy, the majority of work with THOR has predominantly been conducted in high-speed frontal impacts. Previous work conducted (Yuen et al. 2003) showed the rear impact biofidelity of THOR to be much better than the Hybrid III dummy but not as good as the BioRID dummy. The main concern with the THOR dummy was that the neck was too stiff and could not achieve a significant level of s-shape. When a dummy neck is too stiff, the acceleration of the torso is transferred to the head, which is considered unrealistic. While tests with a THOR dummy produced a good indication of the concept seat performance, tests with a BioRID would be required to properly evaluate the concept seat design.

CHAPTER 8 - SLED TESTING OF PROTOTYPE 2 WITH A BIORID DUMMY

8.1 INTRODUCTION

Rear impact sled testing of the concept seat with a seated BioRID dummy was conducted to verify the design. The intention was to run a series of tests with the seat in both standard and concept configuration and compare how each seat influences the dummies motion.

8.2 METHODS

Rear impact crash testing of the concept seat was conducted on a non-rebound crash sled at Chalmers University of Technology in Gothenburg, Sweden. The sled was calibrated for a change in velocity (Δv) of 12.5kph and peak acceleration of 70m/s^2 (7.1g).

The concept seat was rigidly mounted to the sled via a custom built frame. The seat was set to align the seatback centreline at both 15 and 25 degrees from the vertical. A BioRID dummy was positioned with an upright driving posture. A digital angle finder was used on a H-Point tool to set the pelvis to 26.5 degrees and the head to 0 degrees for each test. A lap belt was used to restrain the dummy's abdomen.

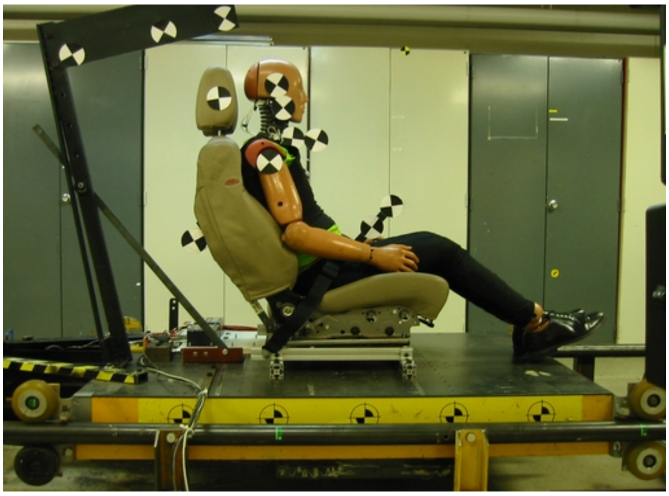

Direction of inbound travel

Figure 8.1: The initially stationary target sled configured for a low-speed rear impact simulation with a BioRID dummy. A rear impact is simulated when a bungee propelled bullet sled impacts a length of flat bar situated laterally across the rear of the target sled. The bar deforms and the impact causes the target sled to accelerate.

Tri-axial accelerometer blocks were used to attach Endevco 2000g accelerometers to the head centre of gravity and T1. An additional accelerometer was attached to the sled to measure the x acceleration. A Brick data acquisition system was used to acquire data at 10 kHz in accordance with SAE J211/1 standards. A Kodak high-speed camera recording at 1000 frames per second was used to record each test for marker analysis and visual inspection. The camera and data acquisition are both triggered by an contact switch on the rear of the sled that is triggered at the time of impact.

Optical markers were applied to several key locations including the head centre of gravity, the chin, T1 via a custom made bracket and the sled (See Figure 8.2). The high-speed video output single images with 1ms intervals. TrackEye software was used to track the optical markers and to conduct depth scaling to account for markers in different planes. The coordinates where then used to calculate the T1 (α), link 1 (β) and link 2 (γ) angles relative to the sled (See Figure 3.3). These angles were then used to calculate the actual change of neck (θ) and head (φ) angles. This procedure was based on techniques developed during the MADYMO modelling study (See 3.5 Methods).

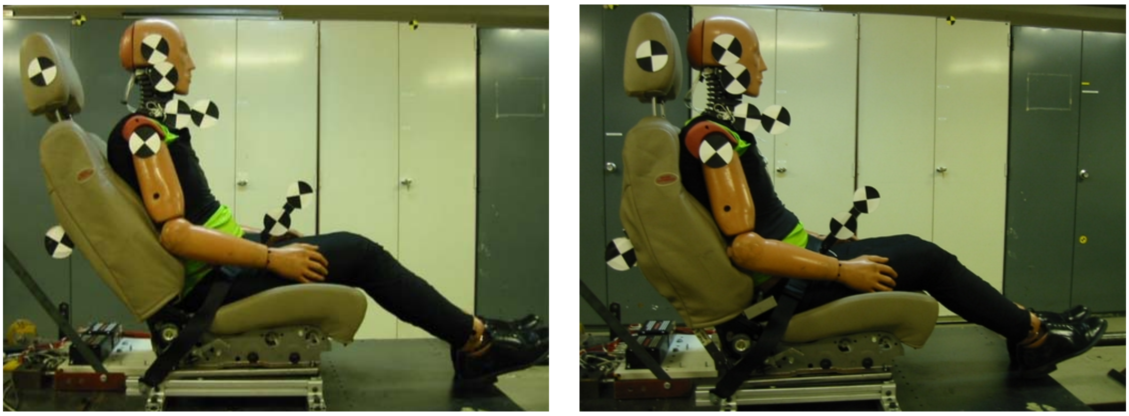

Figure 8.2: A BioRID dummy in the standard seat configuration (left) and the concept seat configuration (right). Note how the concept seat conforms to the dummy and minimizes the initial backset.

Run Name	Seat Configuration	Seatback Angle (deg)	Head Restraint	Sled Pulse (g)	Backset (mm)
std15std	Standard	15	Standard	7	80
std15act	Standard	15	Active	7	80
std25std	Standard	25	Standard	7	140
std25act	Standard	25	Active	7	140
cs15std	Concept	15	Standard	7	40
cs15act	Concept	15	Active	7	40
cs25std	Concept	25	Standard	7	40
cs25act	Concept	25	Active	7	40

Table 8.1: Test matrix for 7g sled tests for standard and concept seat configurations with a standard and active head restraint. The run name is the seat configuration followed by the seatback angle and finally the head restraint configuration. This matrix was chosen to thoroughly evaluate the standard and concept seat both with a standard and active head restraint. Two angles were chosen to show that as seatback angle increases, the standard seat safety decreases while the concept seat safety remains constant.

8.3 RESULTS

This section contains results for a series of 7g sled tests. Both the standard seat (std) and concept seat (cs) were tested with a standard (s) as well as an active (a) head restraint. Each seat configuration was tested with a 15 degree seat back angle and again with a 25 degree angle.

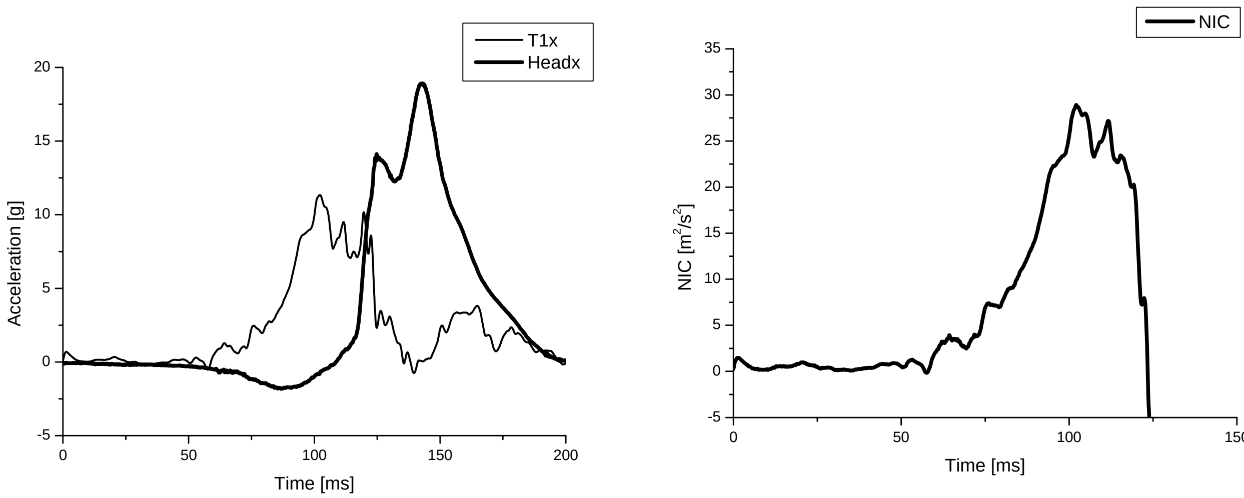

Figure 8.3: Test std15std. Acceleration and NIC results for 7g Prototype 2 standard seat 15 degree test with standard head restraint.

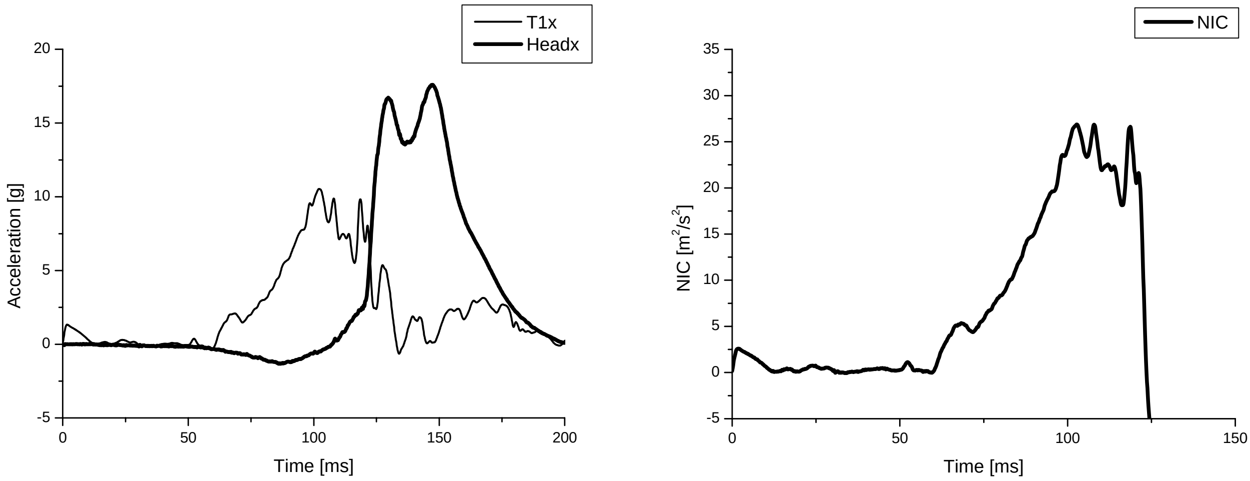

Figure 8.4: Test std15act. Acceleration and NIC results for 7g Prototype 2 standard seat 15 degree test with standard head restraint.

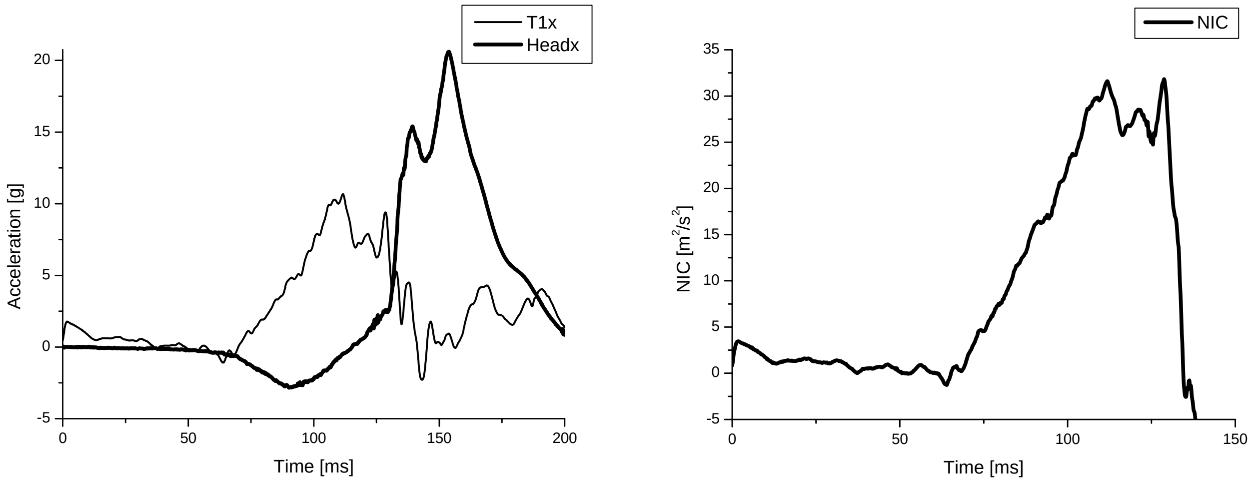

Figure 8.5: Test std25std. Acceleration and NIC results for 7g Prototype 2 standard seat 25 degree test with standard head restraint.

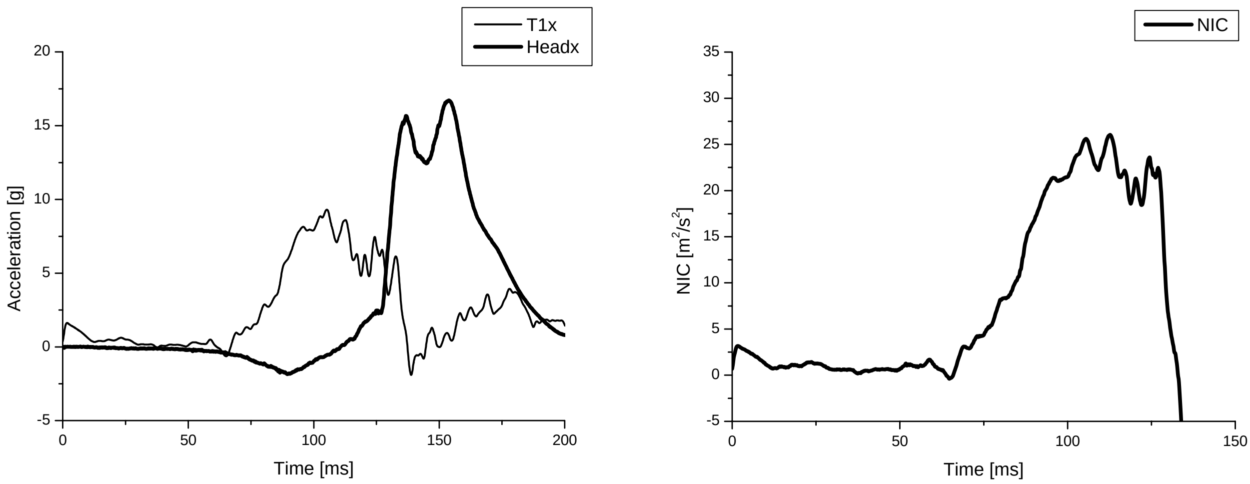

Figure 8.6: Test std25act. Acceleration and NIC results for 7g Prototype 2 standard seat 25 degree test with standard head restraint.

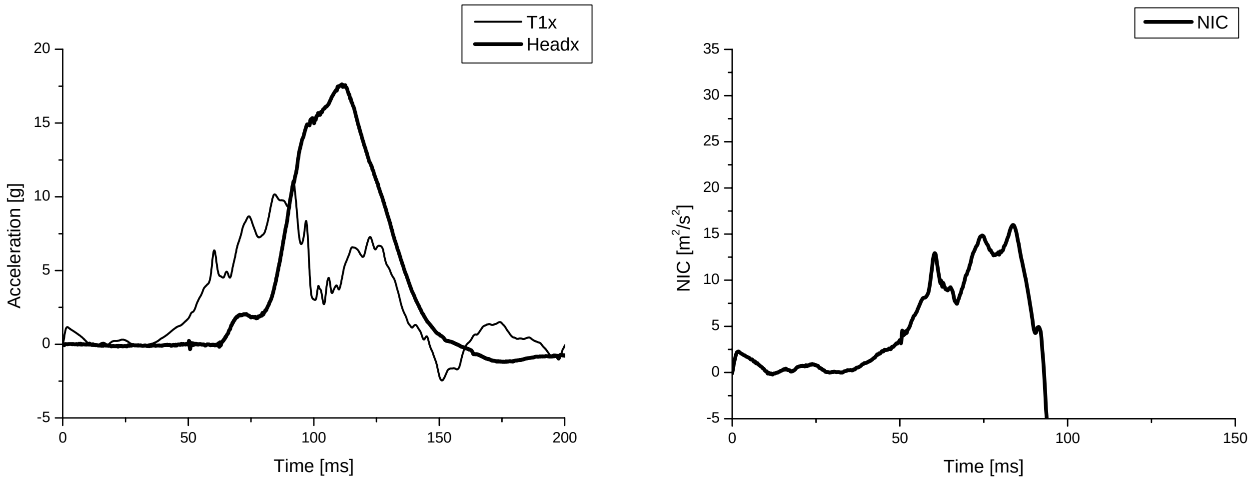

Figure 8.7: Test cs15std. Acceleration and NIC results for 7g Prototype 2 concept seat 15 degree test with standard head restraint.

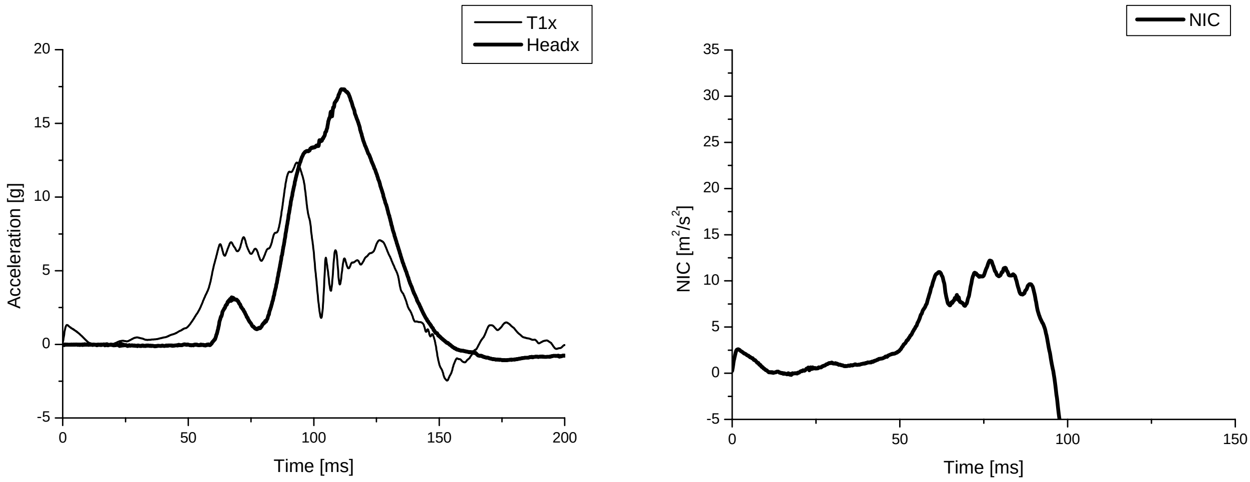

Figure 8.8: Test p2_cs15_a. Acceleration and NIC results for 7g Prototype 2 concept seat 15 degree test with active head restraint.

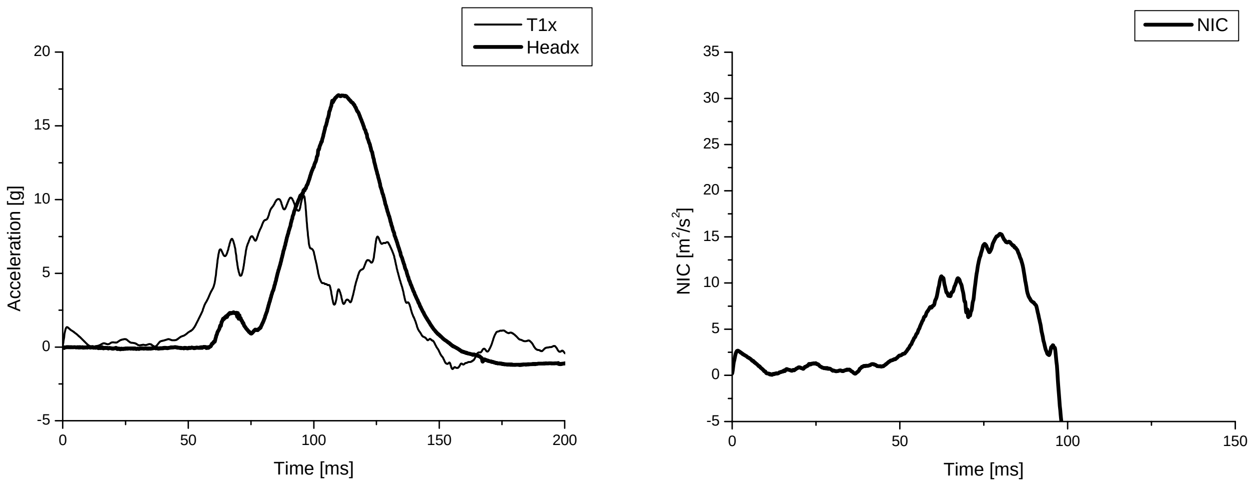

Figure 8.9: Test cs25std. Acceleration and NIC results for 7g Prototype 2 concept seat 25 degree test with standard head restraint.

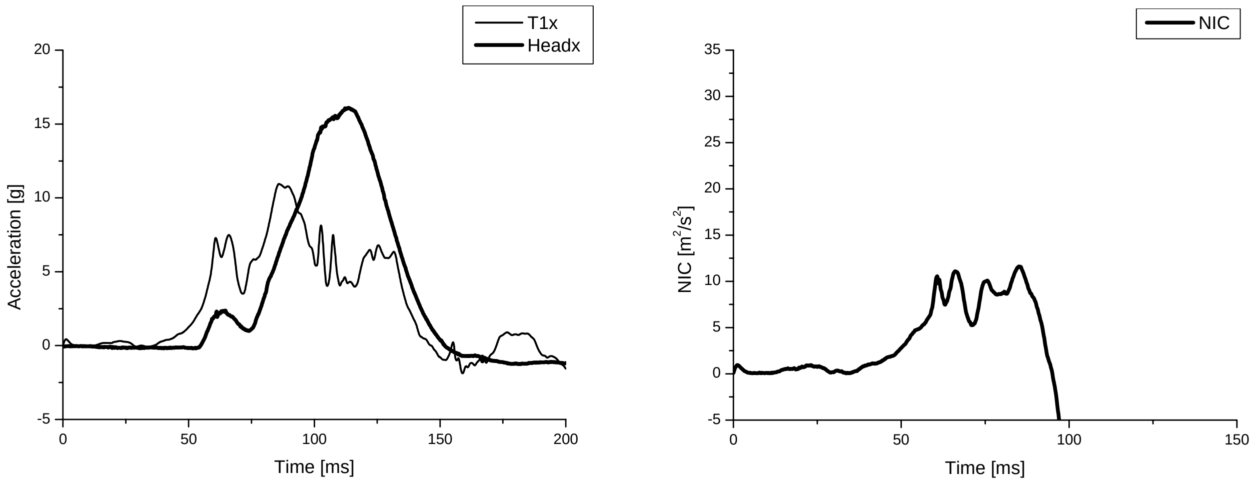

Figure 8.10: Test cs25act. Acceleration and NIC results for 7g Prototype 2 concept seat 25 degree test with active head restraint.

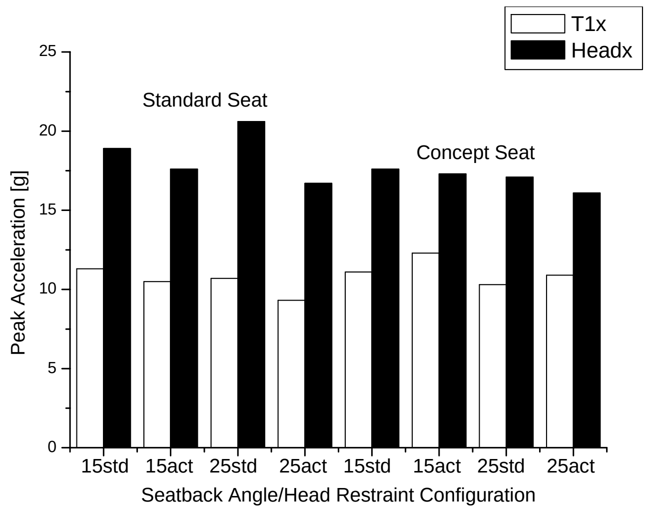

Figure 8.11: Maximum x-acceleration of the head and T1 for each Prototype 2 seat configuration. The concept seat head and T1 accelerations are lower than the standard seat head accelerations.

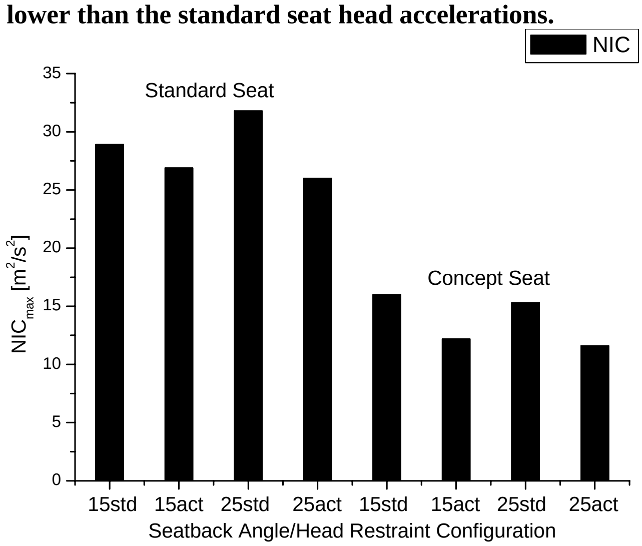

Figure 8.12: Maximum NIC value for each Prototype 2 seat configuration. The concept seat NIC values are lower than the standard seat NIC values. The NIC values are lower for tests with the active head restraint when compared to tests with a standard head restraint. NIC values increase for the standard seat as seat back angle increases while the NIC values for the concept seat remain constant as the seat back angle increases.

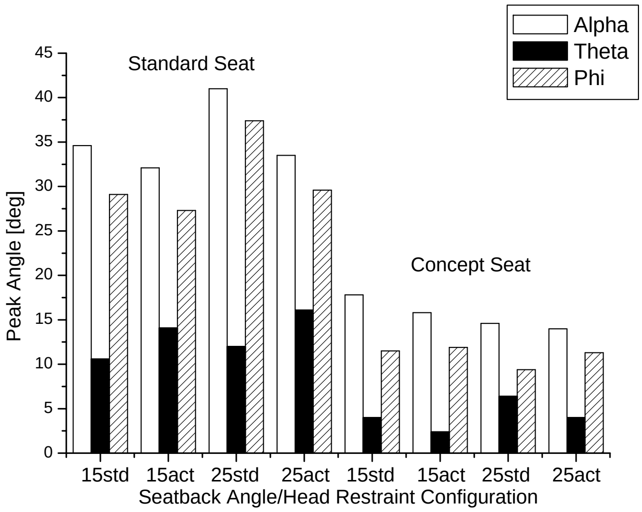

Figure 8.13: The maximum head (φ), neck (θ) and T1 (α) angles for each Prototype 2 seat configuration. Overall, the concept seat angles are lower than the standard seat angles. See Figure 3.3 for angle definitions.

8.2 DISCUSSION

There are three main results to discuss with the Prototype 2 tests: Peak acceleration of the head and T1, maximum NIC values and the maximum head, neck and T1 angles.

The accelerations for head and T1 have been plotted against time for tests std15std, std15act, std25std, std25act, cs15std, cs15act, cs25std and cs25act in Figure 8.3 through to Figure 8.10 respectively. The maximum values have been summarised in a bar graph (See Figure 8.11). For the standard seat with a fixed head restraint the head acceleration for the 15 degree case is 1.7g less than the 25 degree case. The 25 degree case has a larger initial backset and hence the head has more time to translate and rotate in extension hence the higher peak head acceleration. When the active head restraint was used, a significant reduction in peak accelerations for both head and T1 were seen.

For the concept seat with a fixed head restraint the head acceleration for the 15 degree case is 0.3g more than the 25 degree case. Similarly, the T1 acceleration for the 15 degree case is 0.8g more than the 25 degree case. Both peak accelerations are similar in magnitude and this can be explained by the head restraint maintaining a minimised backset at all times. The T1 accelerations are also similar and this is due to the new seatback design that keeps the upper seat back close to the dummy torso at all times. When the active head restraint was used, slight reductions in peak accelerations for both head and T1 were seen. Head and T1 accelerations for the concept seat were slightly lower than the accelerations for the standard seat.

NIC values have been plotted against time for tests std15std, std15act, std25std, std25act, cs15std, cs15act, cs25std and cs25act in Figure 8.3 through to Figure 8.10 respectively. The maximum values have been summarised in a bar graph (See Figure 8.12). For the standard seat with a fixed head restraint the NIC for the 15 degree case is $2.9m^2/s^2$ less than the 25 degree case. When the active head restraint was used, it reduced the NIC by $2m^2/s^2$ for the 15 degree case and $5.8m^2/s^2$ for the 25 degree case. This shows that the standard seat benefits from the addition of an active head restraint.

For the concept seat with a fixed head restraint the NIC for the 15 degree case is $0.7m^2/s^2$ more than the 25 degree case. When the active head restraint was used, it reduced the NIC by $3.8m^2/s^2$ for the 15 degree case and $3.7m^2/s^2$ for the 25 degree case. This shows that the concept seat significantly benefits from the addition of an active head restraint.

The NIC values for the concept seat were significantly lower than the NIC values for the standard seat (See Figure 8.12). While the peak accelerations contribute to the NIC values, it is also important to compare the time difference between the start of both the head and T1 acceleration. The relative acceleration of the NIC equation (See Equations 1-3) is the difference between the T1 and head acceleration. For the standard seat cases the head acceleration (See Figure 8.3 and 8.6) commences during the T1 pulse and continues after the T1 pulse has returned to zero. For the concept seat cases the head and T1 acceleration pulses (See Figures 8.7-8.10) occur within the same range of time. The result is a more uniform acceleration of the head and torso and hence lower NIC values for the concept seat. This result is primarily due to the minimised backset as well as the minimised torso to seat back distance.

Peak angles for the head, neck and T1 have been plotted for tests std15std, std15act, std25std, std25act, cs15std, cs15act, cs25std and cs25act have been plotted in a bar graph (See Figure 8.13). Alpha, beta, theta, gamma and phi represent T1, link 1, neck, link 2 and head angle respectively (See Figure 3.3). For the standard seat with a fixed head restraint the peak angles for the 15 degree case are lower than the peak angles for the 25 degree case. When the active head restraint was used, peak angles for the 15 degree case are lower than the peak angles for the 25 degree case. Both cases with the active head restraint showed lower peak angles when compared to the fixed head restraint cases. This shows that the standard seat benefits from the addition of an active head restraint. For the concept seat with a fixed head restraint the peak angles for the 15 degree case are similar to the peak angles for the 25 degree case. Similarly when the active head restraint was used, the peak angles for the 15 degree case are similar to peak angles for the 25 degree case.

The peak angles for the concept seat were significantly lower than the peak angles for the standard seat (See Figure 8.13). The lower peak angles are due to the minimised initial backset (See Table 8.1), which limits the amount of head, neck and T1 motion. In addition, when the torso loads the seatback it activates the new seatback design and maintains an upright upper seatback and optimal head restraint position.

Overall, the results showed a good correlation between the maximum acceleration of the head and T1, the maximum NIC values and peak head, neck and T1 angles. In all standard seat tests the 25 degree case performed worse than the 15 degree case. This was due to the increased backset associated with the increased seatback angle and fixed head restraint as well as the torso pushing the seatback, and in turn head restraint, further away from the head. It was observed that during a rear impact, the torso would load the seat back and cause an increase in seatback angle and hence force the head restraint to move away from the rear of the head causing an increased back set.

In all concept seat cases both the 15 degree and 25 degree results were similar. These results show that the concept seat not only reduces overall injury potential, but does so irrespective of initial seat back angle. The effectiveness of the new seatback design in the concept seat was evident in the minimised backset through out the rear impact simulation.

For a 15 degree standard seat with a fixed head restraint the NIC value was reduced by 6.9% when an active head restraint was implemented. The new seatback design with a fixed head restraint reduces the NIC value by 44.6%. Similarly for the 25 degree standard seat with a fixed head restraint where the use of an active head restraint reduces the NIC value by 18.24% while the new seatback design reduces the NIC value by 51.9%. When the active head restraint is used with the new seatback design the NIC values are reduced by 57.8% for the 15 degree seatback angle and 63.5% for the 25 degree seatback angle. These results clearly show the whiplash reduction potential of the new seatback design and that the reduction from the new seatback design is much larger than that offered by the existing active head restraint system.

The main advantage of using a BioRID dummy over the THOR is the improved biofidelic response during rear impact. It was possible to adjust the initial position of BioRID with a human-like posture with a slouched spine. During a rear impact the spine would straighten and the neck would develop an s-shape (See Figure 1.1) as seen in human volunteer data. The rear thoracic spine of the BioRID dummy is covered in a silicon skin moulding while the THOR consists of a vest covering a rib cage. The BioRID design also enables a realistic ramping action to occur. For these reasons the BioRID results are consider more realistic than the THOR results.

CHAPTER 9 - DISCUSSION

The aim of this project was to develop an anti-whiplash car seat. The design was based on the idea that the extent of whiplash injury can be reduced by controlling the differential motion between the head and T1. The initial idea was to develop a car seat with an active head restraint to control the motion of the head and neck relative to T1. Through the MADYMO study (See Chapter 3) it became apparent that a seated occupant with a minimised initial backset prior to impact is still likely to experience a whiplash injury. The reason for this is that during a rear impact, the torso loads the seatback and causes it to rotate rearward and hence forces the fixed head restraint away from the head. This allows the head to translate and rotate further than expected. Head and T1 acceleration plots revealed the time lag between the start of T1 and start of head acceleration. This time lag heavily influences the NIC value, which correlates with peak head, neck and T1 angles. The initial seatback angle is also important. While an upright seatback angle will provide some level of support, a more reclined seatback angle increases the distance between the torso and upper seatback and encourages upper torso translation and rotation.

By designing a concept seat that minimises backset and torso to seatback gap during a rear impact, it was hypothesised that a reduction in injury potential could be achieved (See Chapter 2). A concept seat was designed and constructed in MADYMO (See Chapter 3) and a THOR dummy model was used to represent the occupant. Rear impact simulations were conducted to analyse the relationship between the seat and occupant. The seat geometry was modified in an attempt to minimise head, neck and T1 acceleration, NIC and kinematics. The final design showed a drastic reduction in dummy motion over a standard seat model.

The concept seat was built by modifying the seatback and head restraint of an existing production seat (See Chapter 4). The new seatback design keeps the upper seatback within close proximity to the upper torso. A modular design was used to enable the new seatback design to be removed and allow the seat to be configured as a standard seat. An active head restraint mechanism was incorporated into the design, which allowed rearward torso translation into the seatback to activate a mechanism to position the head restraint further forward and upward. This mechanism could be locked to revert the head restraint design to a standard configuration. These features made it possible to have four different seat configurations in one seat. A standard seat with and without an active head restraint and a concept seat with and without an active head restraint.

A THOR dummy was used for sled testing of Prototype 1 (See Chapter 5). Analysis of head, neck and T1 accelerations, NIC values and kinematics revealed that the injury potential could be reduced significantly by maintaining an optimal head restraint and seatback position during an impact. The design was then refined and Prototype 2 was constructed (See Chapter 6 and 7).

The seat was sled tested with a THOR and a BioRID dummy. The THOR dummy results provided an indication of the advantages of the concept seat over the standard seat. Through the use of a BioRID dummy the potential of displaying the safety benefits of the concept seat over a standard seat become more apparent.

Comparison of the NIC values (See Figure 7.10 for THOR and Figure 8.12 for BioRID) and the peak angles for the standard seat against the concept seat (See Figure 7.11 for THOR and Figure 8.13 for BioRID) show a significant reduction in injury potential for the concept seat over the standard seat. These improvements are directly due to a constantly minimised backset and torso to seatback gap, which results directly from the new seatback design and active head restraint being incorporated into the concept seat design.

Results from sled tests with a BioRID dummy showed the NIC value for a 15 degree standard seat with a fixed head restraint was reduced by 6.9% with the implementation of an active head restraint. When the new seatback design was used it reduces the NIC value by 44.6%. Similarly for the 25 degree standard seat where the use of an active head restraint reduces the NIC value by 18.24% while the new seatback design reduces the NIC value by 51.9%. When the active head restraint is used with the new seatback design the NIC values are reduced by 57.8% for the 15 degree seatback angle and 63.5% for the 25 degree seatback angle. These results clearly show the whiplash reduction potential of the new seatback design. Moreover, the magnitude of the injury risk reduction offered by the new seatback is approximately 3-6 times greater than the injury risk reduction offered by the active head restraint.

This new seatback design offers great potential for reducing the risk of whiplash injuries in rear impact collisions. Further development of the seat concept should be carried out with a view to introducing production versions of the seat design into Australian motor vehicles.

REFERENCES

Aldman, B. (1986). 'An Analytical Approach to the Impact Biomechanics of Head and Neck'. Proceedings of the 30th Annual AAAM Conference, 439-454.

Bogduk, N. and A. Marsland (1988). 'The Cervical Zygapophyseal Joint as a Source of Neck Pain'. Spine 13(6), 610-617.

Bostrom, O., Y. Haland, R. Fredriksson, M. Svensson and H. Mellander (1998). 'A Sled Test Procedure Proposal to Evaluate the Risk of Neck Injury in Low Speed Rear Impacts using a New Neck Injury Criterion (NIC)'. 16th Conference on the Enhanced Safety of Vehicles, 1579-1585.

Bostrom, O., M. Y. Svensson, B. Aldman, H. A. Hansson, Y. Haland, P. Lovsund, T. Seeman, A. Suneson, A. Saljo and T. Ortengren (1996). 'A New Neck Injury Criterion Candidate - Based on Injury Findings in the Cervical Spinal Ganglia After Experimental Neck Extension Trauma'. Proceedings of the 1996 International IRCOBI Conference on the Biomechanics of Impact, 123-136.

Davidsson, J., P. Lovsund, K. Ono and M. Y. Svensson (1999). 'A Comparison Between Volunteer, BioRID P3 and Hybrid III Performance in Rear Impacts'. Proceedings of the 1999 International IRCOBI Conference on the Biomechanics of Impact, 165-178.

Eichberger, A., H. Steffan, B. Geigl, M. Y. Svensson, O. Bostrom, P. L. Leinzinger and M. Darok (1998). 'Evaluation of the Applicability of the Neck Injury Criterion (NIC) in Rear End Impacts on the Basis of Human Subject Tests'. Proceedings of the 1998 International IRCOBI Conference on the Biomechanics of Impact, 321-334.

Jakobsson, L., B. Lundell and B. Alfredsson (1998). 'Protecting Against Whiplash in Rear-End Collisions'. Volvo Technology Report No 1, 1-18.

Jakobsson, L. and H. Norin (2002). 'Suggestions for Evaluation Criteria of Neck Injury Protection in Rear-End Car Impacts'. Traffic Injury Prevention 3(3), 216-223.

Muser, M. H., H. Zellmer, F. Walz, W. Hell and K. Langwieder (2001). 'Test Procedure for the Evaluation of the Injury Risk to the Cervical Spine in a Low Speed Rear End Impact'. ETH, GDV and Autoliv, 1-12.

Philippens, M., H. Cappon, M. v. Ratingen, J. Wismans, M. Svensson, F. Sirey, K. Ono, N. Nishimoto and F. Matsuoka (2002). 'Comparison of the Rear Impact Biofidelity of Biorid II and Rid2'. Stapp Car Crash Journal 46, 461-476.

Rangarajan, N., R. White, T. Shams, D. Beach, J. Fullerton, M. Haffner, R. E. Eppinger, H. Pritz, D. Rhule, D. Dalmotas and E. Fournier (1998). 'Design and Performance of the THOR Advanced Frontal Crash Test Dummy Thorax and Abdomen Assemblies'. 16th Conference on the Enhanced Safety of Vehicles, 1999-2010.

Svensson, M. Y., B. Aldman, H. A. Hansson, P. Lovsund, T. Seeman, A. Suneson and T. Ortengren (1993). 'Pressure Effects in the Spinal Canal during Whiplash Extension Motion: A Possible Cause of Injury to the Cervical Spinal Ganglia'. Proceedings of the 1993 International IRCOBI Conference on the Biomechanics of Impact, 189-200.

Viano, D., C. (2001). 'The Effectiveness of Active Head Restraint in Preventing Whiplash'. Journal of Trauma 51(5): 959-969.

Yuen, M. and L. E. Bilston (2003). 'Evaluation of a THOR Dummy in Rear Impact Sled Tests'. Proceedings of the 2003 Road Safety Research, Policing and Education Conference.

GLOSSARY

Active head restraint – A mechanism that optimises head restraint position during rear impact.
Backset – The horizontal distance between the rear of the head and head restraint.
BioRID Dummy – Specialist rear impact dummy developed by Chalmers University of Technology, Sweden.
Crash sled – Test device used to simulate a typical crash.
Head restraint – Foam padded device mounted to the top of a seat designed to protect the head during a rear impact collision.
Hybrid III Dummy – High-speed frontal dummy developed by General Motors.
MADYMO – Mathematical Dynamic Modelling software used for crash simulation.
NIC – Neck Injury Criterion used to compare relative motion between the torso and head.
Ramping – Describes the motion of the occupant sliding upwards relative to the seatback.
Recliner – A mechanism used to adjust the angle between the seat base and seat back.
Seatback – The back part of the seat that supports the torso and connects the seat base to the head restraint
Sled pulse – Acceleration versus time history of a crash sled.
T1 – The first thoracic vertebra, the base of the neck.
THOR Dummy - Test Device for Human Occupant Restraint. Developed by GESAC for the National Highway Traffic Safety Administration.
Whiplash – Describes the motion of an occupants head, neck and torso during an impact. Injury is mainly to soft tissue such as disks, muscles and ligaments.